3-21-2019

Manufacture of Fused Deposition Modeling Joints using ULTEM 9085

Zane A. Willburn

MANUFACTURE OF FUSED DEPOSITION MODELING JOINTS USING ULTEM 9085

THESIS

Zane A. Willburn, Second Lieutenant, USAF

AFIT-ENY-MS-19-M-252

DEPARTMENT OF THE AIR FORCE
AIR UNIVERSITY

AIR FORCE INSTITUTE OF TECHNOLOGY

Wright-Patterson Air Force Base, Ohio

AFIT-ENY-MS-19-M-252

MANUFACTURE OF FUSED DEPOSITION MODELING JOINTS USING ULTEM 9085

THESIS

Presented to the Faculty

Department of Aeronautical Engineering

Graduate School of Engineering and Management

Air Force Institute of Technology

Air University

Air Education and Training Command

in Partial Fulfillment of the Requirements for the

Degree of Master of Science in Aeronautical Engineering

Zane A. Willburn, B.S.M.E.

Second Lieutenant, USAF

21 March 2019

AFIT-ENY-MS-19-M-252

MANUFACTURE OF FUSED DEPOSITION MODELING JOINTS USING ULTEM 9085

Zane A. Willburn, B.S.M.E.
Second Lieutenant, USAF

Committee Membership:

Dr. Carl R. Hartsfield
Chair

Dr. Anthony N. Palazotto
Member

Maj. Ryan P. O'Hara, PhD
Member

Abstract

The manufacture of joints between a base structure and a structure manufactured via Fused Deposition Modeling (FDM) will be investigated. ULTEM 9085, a high temperature plastic with potential aerospace applications, will be the material used. The specific application this research is focused on is a robotic and mobile FDM printer capable of building structures onto other structures in space. A joint will be formed by fusing the base layer of the printed structure and the top of the base structure together. Tensile testing will be performed to determine the strength of the bond between parts. Tensile specimens will be manufactured with variable printer settings, including air gap and build volume temperature. In the orbital environment, lamps could be used to heat the part in place of a heated build volume. A thermodynamic model is used to estimate power required to heat the printed part in vacuum.

In addition, tensile and compression testing will be done on parts printed in various orientations to validate material properties. The material properties of specimens manufactured under normal conditions will be the standard that printed joints will be compared against.

Acknowledgments

I would like to thank my advisor and the numerous laboratory technicians that made this thesis possible.

Zane A. Willburn

Table of Contents

Page

List of Figures

List of Tables

List of Symbols

α	Absorptivity
ϵ	Emissivity
σ	Stefan-Boltzmann Constant
A_c	Cross-Sectional Area
A_s	Surface Area
C_p	Specific Heat
T_0	Initial Temperature
T_∞	Environmental Temperature
h	Convection Coefficient
k	Thermal Conductivity
P	Perimeter of Printed Part
T	Temperature
x	Length
y	Width
z	Height

MANUFACTURE OF FUSED DEPOSITION MODELING JOINTS USING ULTEM 9085

I. INTRODUCTION

1.1 Background

Everything loaded onto a space vehicle must be designed to survive the launch environment. The payload is subjected to quasi-static acceleration loads and vibrations during launch. As a result, the payload structure is more robust than its operational tasks require. The loads that space vehicle structures must support in orbit are low due to micro-gravity. If these structures could be manufactured in orbit, rather than on Earth, the structure would not have to possess the strength to withstand launch and could be made lighter.

Additive manufacturing (AM) may provide a feasible solution to this problem. A robotic and mobile 3D printer could build structures onto other structures in space (see Figure 1.1) . One of the problems presented by this concept is the strength of the bond or attachment between the pre-existing structure and the new 3D printed structure. Parts of the concept have already been proven, such as using additive manufacturing techniques in micro-gravity.

The National Aeronautics and Space Administration (NASA) has shown interest in AM because it allows parts to be manufactured in space rather than launching them from Earth [1]. A potential use of AM technology for NASA is relying on AM for replacement parts. This can reduce launch mass by reducing the number of spare parts required to be launched in a mission [1]. In 2014, NASA launched the 3D printing in

Zero-G technology demonstration to the International Space Station [1]. This mission focused on the ability of the Fused Deposition Modeling (FDM) process to produce parts in the micro-gravity environment [1]. The results of the demonstration indicated that FDM parts manufactured in orbit are similar in strength to parts manufactured on Earth.

FDM is one method of AM that builds parts up layer by layer [2]. The FDM method is one of the most commonly used AM methods. The FDM process requires a 3D model from computer-aided design (CAD) software, and the geometry is broken up into triangles before printing [3]. During the FDM process, the material is fed through a heating element and extruded through a nozzle [3]. The material at this stage is in a semi-molten state, allowing it to fuse to the material it comes into contact with [3]. The print head normally moves in the x-y plane and the platform moves vertically, allowing three-dimensional objects to be made by layering the material [3].

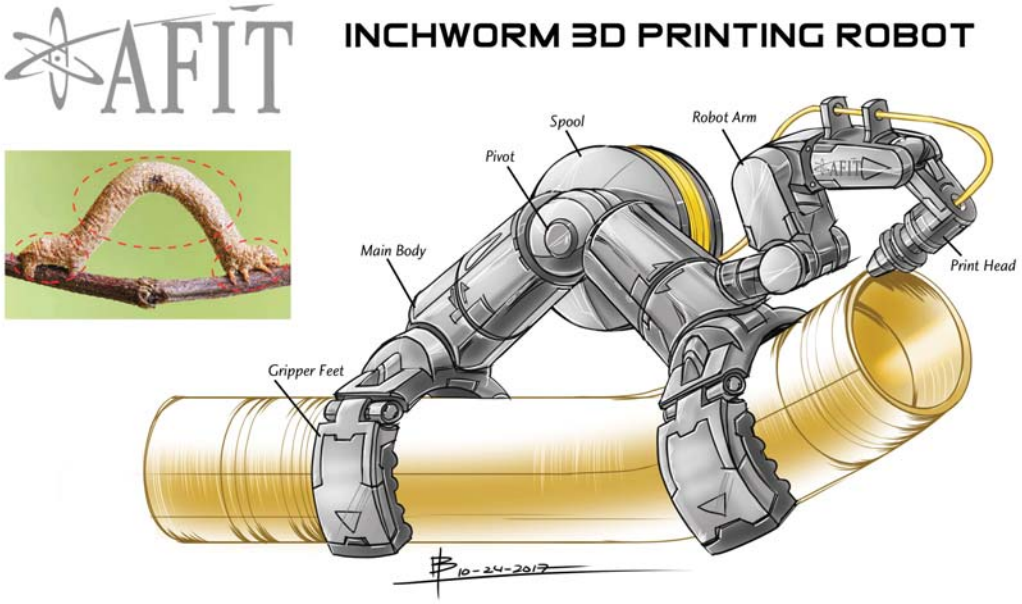

Figure 1.1. Inchworm robot concept art.

1.2 Problem Statement

AM is of interest to the space community for use in producing structures in orbit. ULTEM 9085 is a material with high strength, high temperature resistance, and low out-gassing properties that make it a great candidate for space applications. To implement ULTEM 9085 for use in space, the strength of the attachment between the printed structure and the base structure must be considered. This research will address the strength of joints constructed from ULTEM 9085 using FDM.

1.3 Assumptions/Limitations

Out of the numerous methods of AM, NASA selected FDM to be tested in the in-space manufacturing (ISM) project. The ISM project produced successful test specimens using FDM in orbit. As a result, FDM was chosen in this experiment to further investigate the feasibility of using FDM in space applications. ULTEM 9085 appears to be the most promising material for use in FDM while in the space environment due to its desirable out-gassing properties.

1.4 Scope

This research focuses on creating joints between a pre-existing base structure and a new, fixed structure manufactured using ULTEM 9085 and the FDM method. The method of attachment is fusing the base layer of the new structure to the pre-existing layer using FDM. The results will help determine feasibility of using ULTEM 9085 to print fixed structures on pre-existing structures in orbit using FDM.

1.5 Standards

There is no International Standards Organization (ASTM) standard for AM tensile specimens so ASTM D638-14, Standard Test Method For Tensile Properties of Plastics, will be used as a reference. An ASTM dogbone specimen will be used to validate the tensile properties of ULTEM 9085 in three print directions and using different printers. To test the strength of attachment between a pre-existing structure and a new structure, a non-ASTM specimen was designed. ASTM D695-15 will be used in the testing of compression specimens.

1.6 Research Objectives

This research aims to determine feasibility of printing a fixed structure onto a pre-existing structure using ULTEM 9085. Specifically, the strength of the attachment between the pre-existing structure and the new fixed structure will be investigated. Printing a new structure on a pre-existing structure will be referred to as the composite print method. The following have been identified as research objectives: validate ULTEM 9085 mechanical properties and determine the strength of joints manufactured using the composite print method.

1.6.0.1 Validate ULTEM 9085 mechanical properties

The mechanical properties of ULTEM 9085 will be tested using specimens printed in three different orientations. These specimens will be made by Stratasys and on the Fortus 450mc at the Air Force Institute of Technology (AFIT). Tensile and compression tests will be performed to obtain the mechanical properties of the specimens. These data will be compared against other results, such as the results obtained by Bagsik *et al.* [4].

1.6.0.2 Strength of Joints Manufactured Using the Composite Print Method

First, control column specimens will be manufactured using a Fortus 450mc. These columns manufactured from a single print will provide a baseline for the composite column specimens. Next, specimens will be manufactured by printing half of a composite specimen on a pre-existing half part. The pre-existing halves will be printed using the Fortus 450mc. Specimens will be completed using a Fortus 450mc or modified LulzBot TAZ 6 by printing ULTEM 9085 onto the pre-existing part. Specimens will then undergo tensile testing to determine the strength of the attachment between the two structures. Printing ULTEM 9085 on a pre-existing structure manufactured using ULTEM 9085 is the method of attachment (the composite print method). The temperature of the build volume will be varied to test its effect on the attachment between new and pre-existing layers.

1.7 Materials and Equipment

The following equipment will be used:

1. Stratasys Fortus 450mc, for printing specimens
2. Modified LulzBot TAZ 6, for printing specimens
3. MTS Landmark Servohydraulic Test System, for tensile testing
4. MTS 810 with a 110 kip load frame, for compression testing
5. Zeiss microscope, for observing specimens
6. ULTEM 9085 Feedstock

1.8 Other Support

AFIT lab technicians will provide support in the tensile laboratory, printing laboratory, and microscope laboratory.

1.9 Thesis Overview

- Chapter 1: Provides a problem statement, assumptions, scope, standards, objectives, materials and equipment, and other support
- Chapter 2: Provides background in space based AM and need for characterization of joints between pre-existing structures and new fixed structures. Also includes literature review
- Chapter 3: Discusses methodology for experimentation and data
- Chapter 4: Analyzes test results and discusses feasibility of printing new fixed structures on pre-existing structures
- Chapter 5: Summarizes results and discusses recommendations for future research

1.10 Summary

There are many aerospace applications for components built with ULTEM 9085 using FDM. One specific application is building structures in the space environment onto existing structures using FDM. The joint connecting the new structure and the base structure must be considered. The strength of the joint between a new structure and a base structure will be tested using tensile specimens manufactured with ULTEM 9085 using FDM. The results will help determine the feasibility and requirements for a FDM robot that can be used to build structures in orbit.

II. BACKGROUND

2.1 Chapter Overview

To print a new structure on an existing structure, the FDM process must be understood. There are many variables that may affect the strength of attachment to the first layer of the print. This chapter will provide an overview of what is important to the adhesion and strength of the base layer and work that has been done to determine feasibility of using FDM in the space environment.

2.2 Additive Manufacturing Techniques

According to ASTM F42, "Additive Manufacturing," there are seven categories of additive manufacturing. The first is Vat photopolymerisation. The Vat photopolymerisation technique uses a chamber filled with liquid resin and an Ultraviolet (UV) light. The UV light moves in the x and y directions while the chamber filled with liquid resin moves down in the z direction. The UV light cures the resin and the chamber moves down, constructing each layer upon the previous layer [5].

The next method is material jetting. The material is jetted onto the build plate and the layers are cured using UV light [5]. The material is deposited in drops, so polymers and waxes are most commonly used in the material jetting process [5]. Each layer is built on top of the last.

The third method is binder jetting, also known as 3DP. Most commonly, a liquid binder is used to bind powder layers [5]. Alternating layers of binder and powder build material are built up to form the part. Post processing is often required.

Method number four is material extrusion, or FDM, and will be discussed in detail in Section 2.3.

The fifth method is powder bed fusion, encompassing several types of more specific

techniques. A laser or electron beam is used to melt powder and fuse the material together [5]. After a layer has been melted and fused, a new layer of powder is spread on top of the last and then melted and fused to create the next layer.

The sixth method listed in ASTM F42 is sheet lamination. Sheets are placed on the previous layer and cut to size using a knife or laser [5]. Each layer is bonded to the last using an adhesive. Resulting parts are not suitable for structural use [5].

The last method is directed energy deposition (DED), also known as 3D laser cladding. DED is most commonly used to add material to existing parts or for repair [5]. A nozzle mounted on a multi-axis arm deposits material from either a powder or wire.

2.3 FDM Definition and Overview

FDM is a method of AM developed by Stratasys that builds parts by laying down material one layer at a time. The FDM process requires a three-dimensional model from computer-aided design (CAD) software, and the geometry is broken up into triangles before printing [3]. The triangular surfaces are made using a standard tessellation language (STL) file. During the FDM process, the material is fed through a heating element and onto a build plate or onto the last layer extruded from the nozzle [3]. The feedstock is fed through the nozzle by drive gears. There are two common drive systems for the feedstock. Figure 2.1 (a) shows a Bowden drive system, where the drive gears are located near the feedstock hopper. Figure 2.1 (b) is a direct drive system, where the drive gears placed near the print head. The Bowden drive system drives the filament through the nozzle from the hopper while the direct drive system drives the filament through just before the print head. The Bowden drive system allows for a lighter print head, but the feedstock must be prevented from buckling between the drive gears and the hot end [6]. The material is in a semi-molten state as

it is fed through the nozzle, allowing it to fuse to the material it comes into contact with [3]. The print head moves in the x-y plane and the platform moves vertically, allowing three-dimensional objects to be made by layering the material [3]. If there are overhangs of more than 45 degrees, support material may be used to support the part while it is being built.

FDM is the most feasible method for the application of printing structures in space. Most of the other methods listed in Section 2.2 are not desirable due to the form of the build material or the post processing required. Build material in powder or liquid form would be difficult to implement in microgravity, eliminating Vat photopolymerisation and powder bed fusion techniques. FDM is the only method that can be reasonably implemented in a mobile printing unit in microgravity, especially because its feedstock is in wire or filament form.

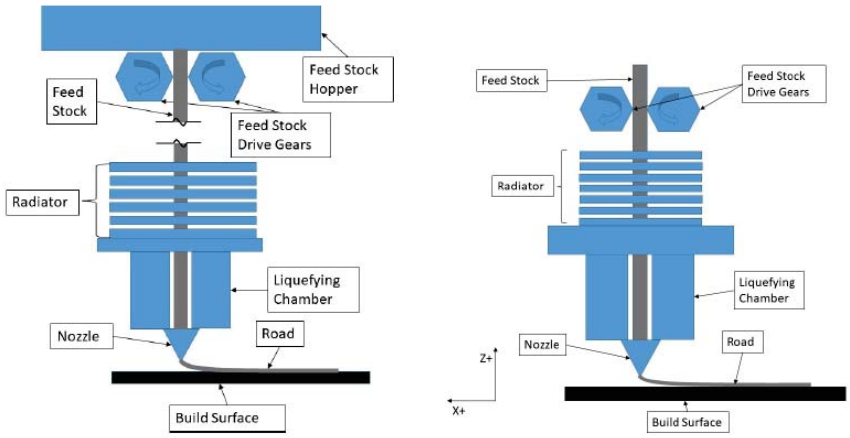

Figure 2.1. (a) Bowden Drive System and (b) Direct Drive System (figures from Cerri *et al.*) [6]

There are many parameters that affect the properties of FDM parts. Parts built using FDM have anisotropic properties that depend on the orientation of the print [3]. The tool path used to form layers can be varied. One common method is a raster fill, where the perimeter of the layer is printed first and then the rest of the layer is

filled by roads normally oriented 45 degrees to the x-axis [4]. The next layer is then filled with a raster in the opposite direction (see Figure 2.2). Figure 2.2 depicts a layer with three perimeter roads and a raster fill in the center.

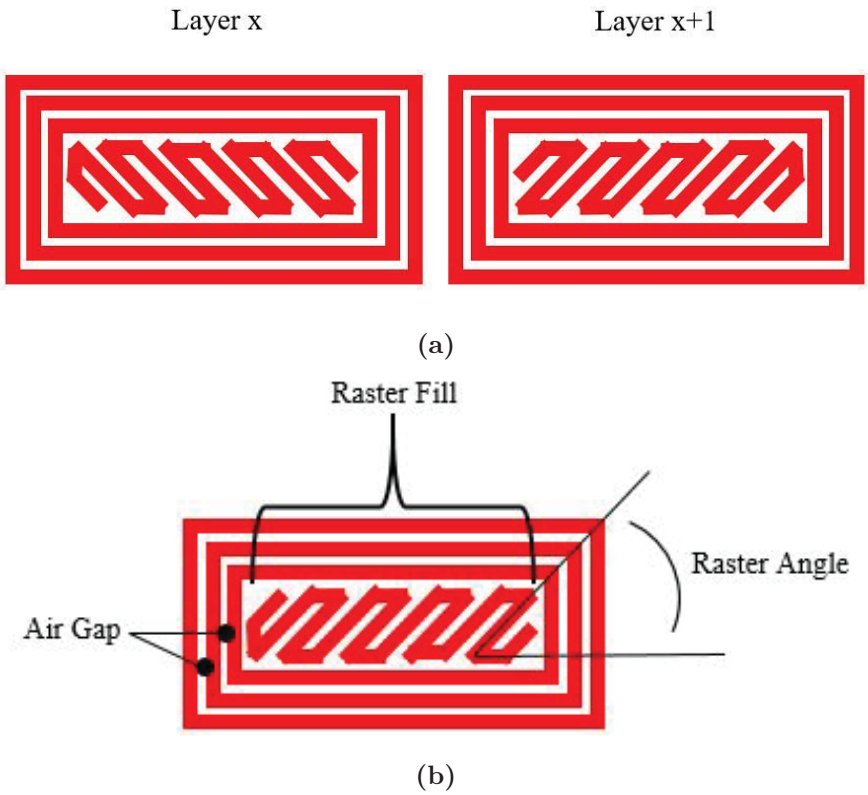

Figure 2.2. (a) Raster fill at 45 degrees (figure re-created from Bagsik *et al.* [4]) (b) Example of a layer cross-section (figure re-created from Gebisa *et al.* [7])

The size of the bead, or road, that is laid down by the nozzle helps determine the part's mechanical properties. The air gap is the gap between roads. The air gap can be adjusted to make roads tightly packed, resulting in a dense part, or set for gaps between roads [3]. It was found that acylonitrile butadiene styrene (ABS) P400 tensile specimens with a negative air gap are stronger than those with zero air gap, and all specimens manufactured via FDM are weaker than injection molded specimens [3].

Temperature also affects part quality. Both the model build temperature and envelope temperature are important in the FDM process. The model build temperature

is the temperature of the heating element that heats the material prior to leaving the nozzle. The envelope temperature is the ambient temperature around the part being printed. Envelope temperature can be controlled by printing parts inside a chamber.

2.4 Material Testing

To characterize mechanical properties, tests can be performed. Mechanical stress must be applied to a part to observe the mechanical behavior [4]. One of the most common materials tests is the tensile test. Tensile test results provide key mechanical properties such as ultimate strength, yield strength, and elastic modulus. In a tensile test, a specimen is normally pulled axially until failure. Tensile specimens normally consist of a grip section and a gage section. The resulting specimen geometry resembles a dog bone (see Figure 2.3). The grip section is used to grip the specimen in the test machine. The gage section is made smaller than the grip section so that most of the reaction to mechanical stress occurs there. The testing machine produces a tensile force on the specimen, and the elongation of the specimen is measured and recorded as force is increased [8]. The relationship between the applied load and deformation can be converted to a stress-strain diagram [8].

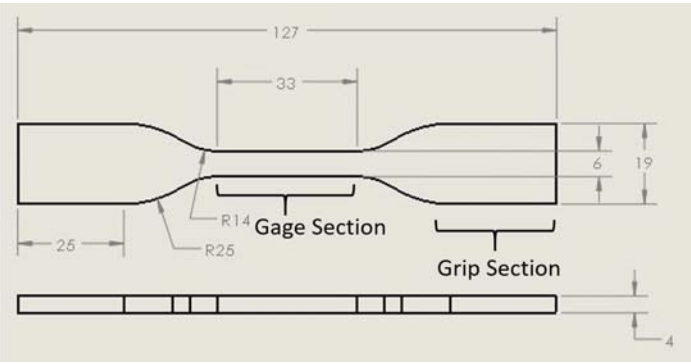

Figure 2.3. Illustration of a type IV dogbone specimen from ASTM D638.

An extensometer can be used to measure the elongation in the test specimen [8]. The extensometer is placed on the gage section of the test specimen (see Figure 2.4).

Two knife-edges are placed in contact with the gage section, and the initial distance between the knife-edges provides the gage length [8]. The specimen will elongate as the applied load is increased, causing an increase in distance between the knife-edges.

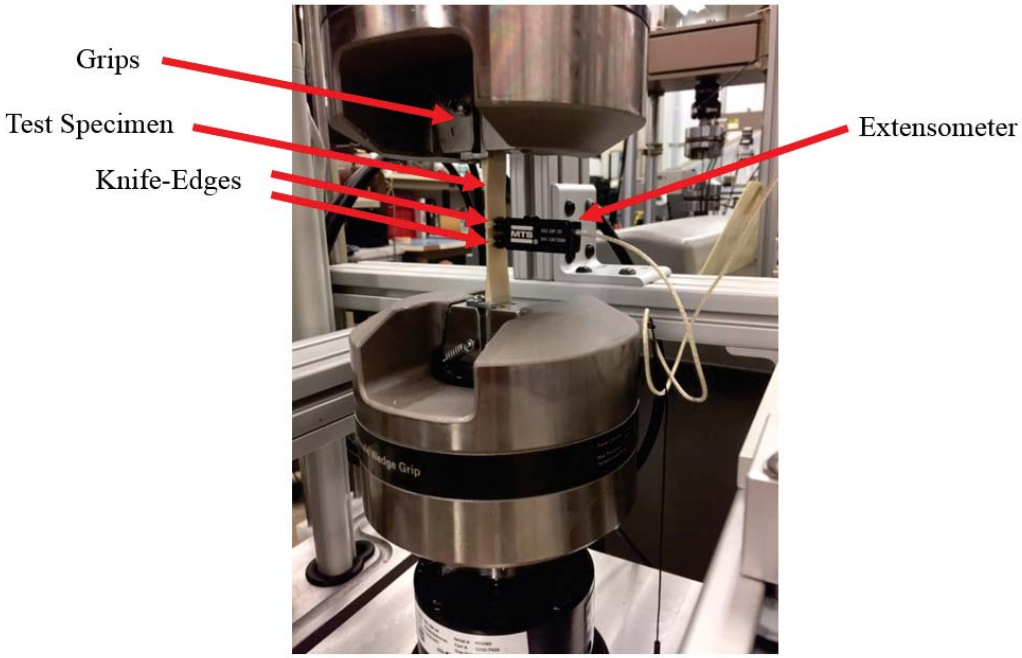

Figure 2.4. Tensile Test Setup with Extensometer

The elastic modulus, or Young's modulus, is the slope of the initial, linear portion of the stress-strain curve [8]. The elastic modulus is a measure of stiffness, meaning it determines how much bending or stretching will occur under load [8]. Yield strength is the stress that will result in permanent deformation of a material and is normally found at the end of the linear portion of a stress-strain curve. Ultimate strength is the peak stress reached on the stress strain curve. These measures of strength are important because they determine how much stress the material can take before permanently deforming and the maximum amount of stress it can withstand.

The ductility of a material can also be determined using a tensile test. A brittle material will yield little before fracture and a ductile material will withstand more

strain before fracture [8] (see Figure 2.5).

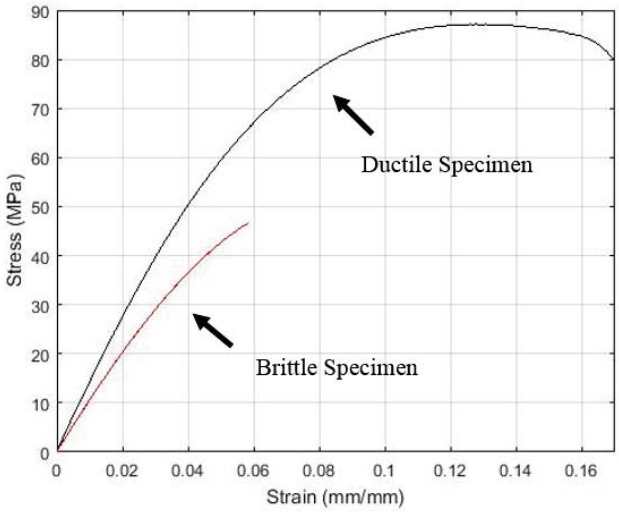

Figure 2.5. Stress Strain diagram of ductile and brittle specimens printed on edge and vertically respectively. Data is from ULTEM 9085 specimens manufactured via FDM.

2.5 Mechanical Properties of ULTEM 9085 Manufactured Using FDM

ULTEM 9085, a type of Polyethermide (PEI), is the material of interest for this project. ULTEM 9085 is a high temperature plastic developed by Stratasys that possesses high strength, high temperature resistance, and desirable out-gassing properties.

out-gassing occurs when gas is released from a material. Polymers can have volatile products used in the manufacturing process trapped inside the material. When the volatile material escapes from the material, it is known as out-gassing [9]. This is most commonly due to high heat, high moisture, or low pressure [9]. In the vacuum of space, the potential for out-gassing is increased. out-gassing is undesirable in the space environment because the volatile products of out-gassing can accumulate on electronic equipment, potentially causing failure of electronic components [9]. Out-gassing can also cause products to accumulate on optics or solar panels, reducing

their effectiveness. Stratasys has completed out-gassing tests on ULTEM 9085 deposited by a Fortus FDM printer [10]. Using ASTM Test Method E 595, it was found that ULTEM 9085 had a total mass loss of 0.41% [10]. NASA's standard for a low out-gassing material is less than 1.0% Total Mass Loss, so ULTEM 9085 is classified as a low out-gassing material.

Stratasys developed ULTEM 9085 to be used in the FDM process to create fully functional parts or prototypes [11]. Certified ULTEM 9085 has unique certifications that meet requirements for aerospace applications. The certification includes test criteria and material traceability. Certified ULTEM 9085 comes with a certificate of analysis for raw material and filament, along with identification for the manufacturing lot number, allowing traceability back to the raw material [11]. These properties make ULTEM 9085 a good candidate for space applications.

One resource for information regarding ULTEM 9085 used in FDM was the work done by Bagsik *et al.* [4]. The FDM part quality of parts made with ULTEM 9085 was investigated, with a focus on print orientation. The print orientation affected both the tensile and compressive properties of the specimens. Specimens were made using a Fortus 450mc. Specimens printed in the X and Z directions have roughly the same elastic modulus, while specimens printed in the Y direction have a lower elastic modulus. X direction specimens had the highest ultimate strength because of a larger plastic region. Specimens printed in the Z direction failed near the yield strength between layers of the print. The X direction specimens had no raster fill, so the tensile stress was parallel to the road direction in the gage section, unlike the Z and Y directions with a raster fill. Bagsik also conducted compression tests of ULTEM 9085 specimens printed in different orientations. Compression specimens printed in the Z direction had the highest compressive strength, meaning that pressing the layers together will support the highest load in compression [4]. The failure of

compression specimens is illustrated in Figure 2.7.

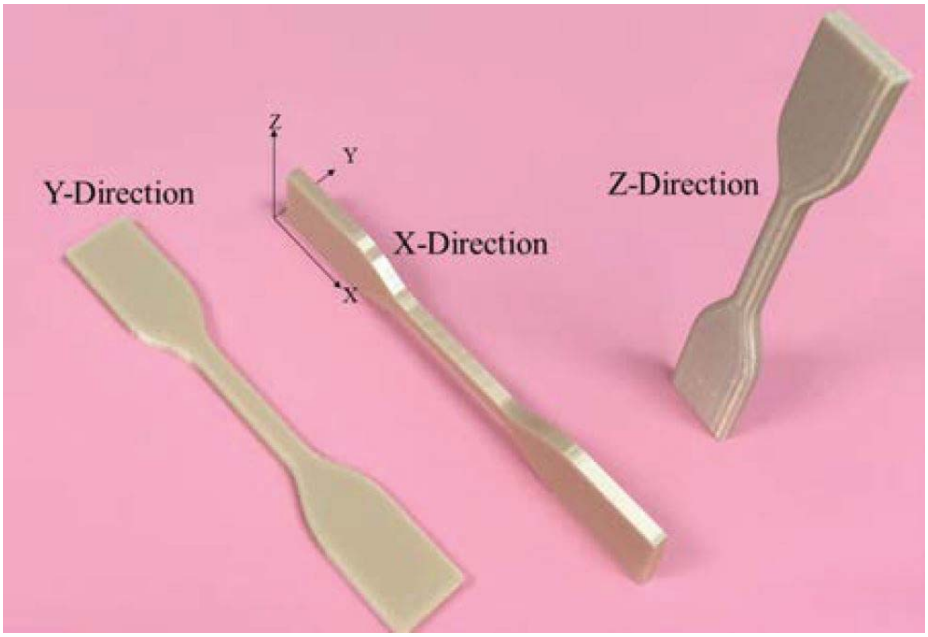

Figure 2.6. Print Orientations used by Bagsik *et al.* [4] (figure from Cerri *et al.* [6])

Table 2.1. Bagsik Print Direction Mechanical Properties (Table taken from Cerri *et al.*

Print Direction (number tested)	X(12)	Y(12)	Z(40)
Tensile Strength (MPa)	63.25 ± 1.07	45.87 ± 1.32	40.71 ± 2.07
Tensile Strain (%)	5.65 ± 0.08	4.99 ± 0.44	2.29 ± 0.19
Tensile Stress at Break (MPa)	61.34 ± 1.31	45.67 ± 1.38	40.75 ± 2.06
Tensile Strain at Break (%)	6.35 ± 0.28	5.0 ± 0.45	2.29 ± 0.19
Elastic Modulus (MPa)	2033.54 ± 64.73	1461.41 ± 194.4	2092.26±129.92

Bagsik *et al.* also tested reproducibility in terms of geometric tolerances of ULTEM 9085 parts made with FDM. Parts were found to have tolerances of 0.05 mm.

Another important consideration for using ULTEM 9085 in the FDM process is the humidity of the filament. Tensile strength was reduced by more than 60% over the range of filament moisture levels tested by Zaldivar *et al.* [12]. Specimens manufactured using filament with more than 0.4% moisture content have poor surface quality compared to those manufactured with filament having a lower moisture content [12]. Image analysis showed an increase in porosity of manufactured parts as moisture con-

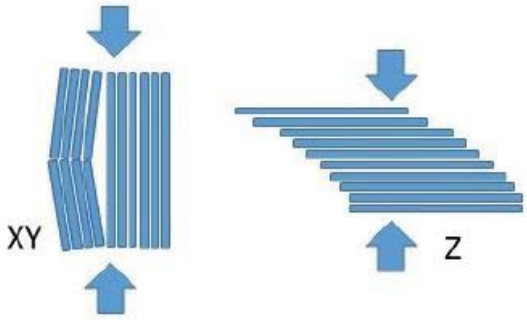

Figure 2.7. Illustration of failure in XY and Z print directions observed by Bagsik *et al.* (figure from Cerri *et al.* [4])

tent of filament was increased above 0.16% [12]. Tensile specimens printed in in the XY direction (flat) with filament containing 0.4% moisture content or more exhibited no plastic deformation, while specimens with a lower moisture content did [12]. In the ZX direction, specimens printed using filament with 0.4% moisture content or more were not suitable for testing due to the poor quality of the specimens [12]. The moisture absorption behavior of ULTEM 9085 filament indicates that the filament will reach unacceptable moisture levels in one hour at room temperature [12].

2.6 Thermal Analysis

Neck formation is one reason the thermal characteristics of a part are important. The portion of two roads that fuse together is known as the neck. This neck is what holds the roads and the resulting part together. Work done by Bellehemeur *et al.* shows good agreement between models and experimental results. The models that assume the properties of the neck are the same as the properties of each individual road [13]. The size of the neck between roads, or filaments, is what Bellehumeur *et al.* used to assess the integrity of the neck. The properties of the neck are driven by the thermal energy of the material being printed. The heat required depends upon several factors, including print speed and the diameter of the roads [13]. As a part is printed, the roads are hot enough to fuse together. The roads then cool and the

bond is complete. Bellehumeur *et al.* also investigated the effect of the envelope and extrusion temperature on neck formation. It was found that both a higher envelope and extrusion temperature results in a larger neck being formed between roads [13]. However, the extrusion temperature has a greater effect on neck formation than the envelope temperature.

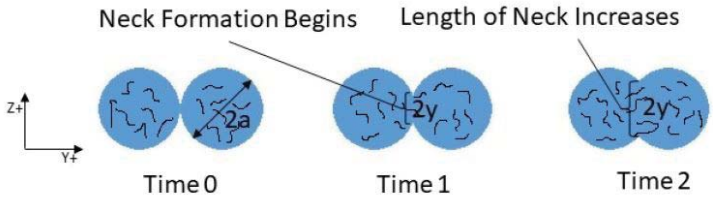

Figure 2.8. Roads fused together forming necks (figure from Cerri *et al.* [6])

Thermal modeling and experimentation of ULTEM 9085 parts manufactured via FDM was accomplished by Cerri *et al.* ULTEM 9085 requires a higher print temperature than other plastics, such as polylactic acid (PLA) (see Table 2.2). The room temperature row refers to the ambient temperature around the part, and the model temperature is the temperature of the material being extruded through the nozzle.

Table 2.2. Thermal table (from Boschetto *et al.* [14])

Material	ABS	ULTEM 9085	Polycarbonate
Room Temperature C°	75	195	145
Model Temperature C°	270	375	342
Support Temperature C°	270	420	330
Prototyping System	Stratasys Bst768	Fortus 900mc	Fortus 400mc

The thermal environment includes the temperature of the heating element and the ambient temperature around the printed part. A thermal model of the space environment using only conduction and radiation was developed by Cerri *et al.* [6]. The model is 1D, steady-state and assumes layer height is equal to nozzle diameter and constant material properties. First, a terrestrial model including convective heat transfer was used. Analysis was done on a hollow cylinder 40mm in height, 50mm in

outer diameter, and 48mm in inner diameter. The cylinder was printed in the modified TAZ 6 and thermal images were taken during the print using a FLIR microbolometer camera. The FLIR images provide experimental temperature to compare the terrestrial model against and aid in calculating power required for heating the printed part in orbit. Fourth order scaling was used to convert the FLIR image intensity to temperatures, along with the assumption that the maximum temperature in the image is the nozzle temperature and the minimum is the build volume temperature. Temperature changes within the small wall thickness and in the nozzle travel direction are neglected. These temperature gradients are small compared to the gradient traveling between layers in the z-direction. Numerical methods matched poorly with experimental data, so a semi-analytic method was used. An energy balance including convection, conduction, radiation, and energy storage terms was calculated. The energy balance along with the estimated direct contribution of radiated energy from the lamps was used to gauge the accuracy of the model. The model was then extended to the orbital environment by removing the convective heat transfer term. Using the model with no convection, the additional power required from lamps to achieve the desired part temperature was calculated [6]. These lamps would heat the part to the desired temperature without a build volume in the orbital environment.

If the temperature of the part is too low, de-lamination will occur and part quality will be reduced. The temperature profile during the printing process was also developed. A FLIR microbolometer camera was used to capture the temperature of the part as it was being printed. Cerri *et al.* produced plots of temperature vs nozzle distance to determine how the rate of road cooling changes with print speed.

More work has been done on interlayer cooling by Morales *et al.* [15]. To simulate building large parts, delays were added between layers. Printing a large part means the nozzle will not return to the same position in the next layer for longer time. A

delay results in more cooling and a reduction in neck formation. ABS was the material used in the testing, and no build volume temperature control was used. As the time delay between layers was increased, the yield strength of the printed compression specimens decreased [15]. The rate of cooling of a completed layer was determined using a FLIR A655sc thermal camera.

2.7 NASA FDM Program in Microgravity

NASA has conducted testing of specimens manufactured in orbit on the International Space Station (ISS) using FDM. The ability for parts to be manufactured in space may allow humans to work in space for longer periods of time [1]. Possible applications for crews in space include part replacing and reducing launch mass by reducing the number of spare parts that must be launched into orbit [1].

The material selected for testing by NASA during the experiment, known as Phase I, is ABS [1]. The testing was completed to determine the feasibility of using FDM in microgravity. The tensile, compressive, and flexural properties of specimens printed on the ground and in orbit were compared. A summary of the results are shown in Table 2.3. "Gravimetric density, ultimate tensile strength, modulus of elasticity, fracture elongation, compressive strength, compressive modulus, flexural strength, and flexural modulus were significantly different for the ground and flight specimens" [1]. The specimens printed in orbit also exhibited a higher variance in geometry. Prater *et al.* provides several hypotheses for these results, one being a problem with the build plate distance from the nozzle. In orbit, the build plate was closer to the nozzle than it was on the ground. This could be the reason why the specimens manufactured in orbit had poorer geometric tolerances and higher density.

Another potential cause of variation between flight and ground specimen mechanical properties is the feedstock. The feedstock has a shelf life of one year, and there

Table 2.3. Summary of tensile specimens printed on the ground and in orbit (from Prater *et al.* [1]). Ground specimens were printed normally on Earth while the flight specimens were printed aboard the ISS in microgravity.

Material Property	Percent Difference (With Respect to Ground)	Coefficient of Variation (Flight) (%)	Coefficient of Variation (Ground) (%)
Ultimate tensile strength (ksi)	17.1	6.0	1.7
Modulus of elasticity (msi)	15.4	6.1	2.7
Fracture elongation (%)	-30.4	26.3	9.9
Compressive strength (ksi)	-25.1	3.1	5.0
Compressive modulus (msi)	-33.3	9.4	4.2
Flexural strength (psi)	25.6	9.3	6.0
Flexural modulus (msi)	22.0	9.6	3.9

was a five-to six-month delay before the feedstock used to manufacture flight specimens was used [1]. Aged feedstock may be more brittle, resulting in specimens of higher strength [1].

The results of NASA's Phase I experiment are promising. While NASA used ABS plastic in the FDM process, other materials may produce similar results. The FDM process for ULTEM 9085 is essentially the same, with the build volume temperature being the biggest difference.

2.8 Summary

FDM can be used with ULTEM 9085 to produce fully functional parts. The mechanical properties of the part depend greatly on print orientation and on the model and envelope temperatures. The capabilities of FDM were also tested by NASA in microgravity to determine the feasibility of printing parts in orbit. The experiment aimed to isolate the effects of microgravity on the FDM process. Specimens printed in orbit were slightly stronger and more dense than those printed on the ground. It is expected that ULTEM 9085 will perform similarly to the ABS that NASA tested aboard the ISS using the FDM process.

Printing in the vacuum of space will present additional challenges, but the work done by Cerri *et al.* [6] presents a reasonable estimate for the power required to achieve the needed part temperature. To the author's knowledge, no work has been done to determine the strength of the joint between a pre-existing part and a newly printed part using ULTEM 9085 via FDM.

III. RESEARCH METHODOLOGY

3.1 Chapter Overview

This chapter explains the research methods used to address each of the research objectives. The first research objective is to validate the mechanical properties of ULTEM 9085 printed using FDM in different print orientations. The second research objective is to test joint strength between a pre-existing part and a newly printed part manufactured via FDM (the composite print method). The results of the testing done on normally printed specimens will be the standard that the composite print method results will be compared against.

3.2 Tensile Specimens

Specimens were manufactured either by Stratasys or at the test location using the Fortus 450mc. The first set of tensile specimens are standard dogbone specimens manufactured to meet specifications for Type IV specimens described in ASTM D638-14, Standard Test Method For Tensile Properties of Plastics (see Figure 3.2). These specimens were printed in the XY, YX, and ZX directions (see Figure 3.1). Printed specimens in these three directions were ordered directly from Stratasys. Specimens were also printed to the same specifications at the test location using the Fortus 450mc. The specimen to specimen variation in width and thickness at the gage section for all these specimens were less than 1%.

The lot number of the ULTEM 9085 feedstock used to manufacture parts was not recorded. All prints completed in the Fortus 450mc used Stratasys Fortus feedstock in both natural and black colors. All prints completed in the TAZ 6 used 3DX Tech 1.75mm feedstock in natural color. Feedstock was fed directly from a PrintDry filament drying system set to 70 C°into the TAZ 6.

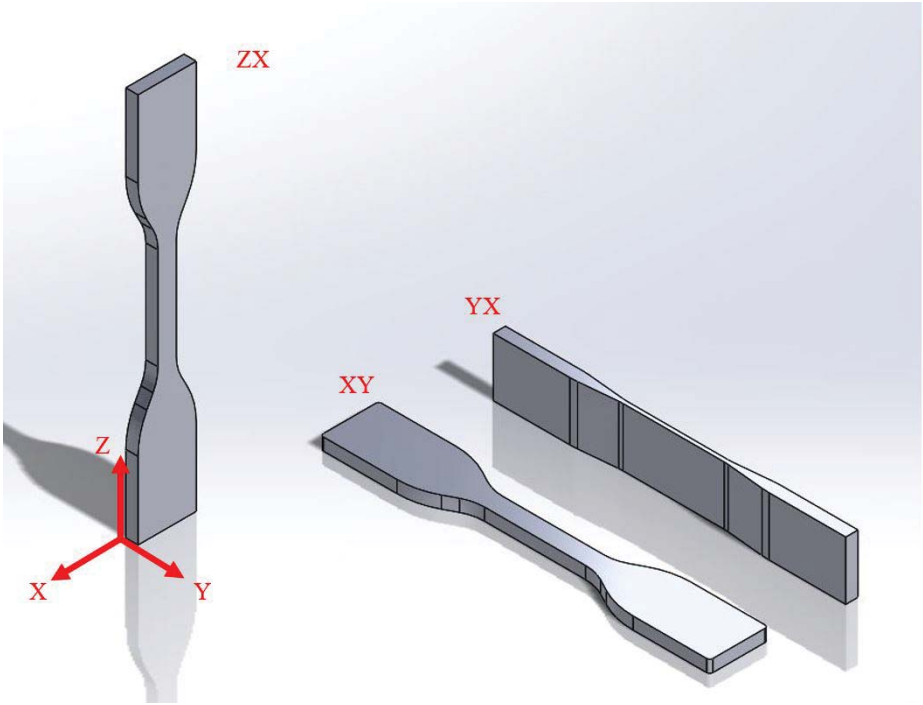

Figure 3.1. Print directions used for tensile specimens.

The settings are fixed for the Fortus 450mc and cannot be changed. Feedstock type is recognized by the Fortus 450mc and the settings are locked in. For ULTEM 9085, the nozzle is set to 375 C°and the build volume temperature is set to 170 C°. Settings for the LulzBot TAZ 6 can be found in Appendix A. The build volume temperature is varied in the TAZ 6.

3.2.1 Column Tensile Specimens

The column specimens are rectangular (8mm x 19mm x 115mm) without a reduced area gage section. The specimens were designed this way for ease of manufacturing. Standard dogbone specimens were considered, but would not provide a large surface area to create a joint in the gage section using the composite print method. A larger surface area means more error is acceptable in aligning specimens. The specimens are rectangular to allow a larger area for the base layer of the newly printed part. Rectangular specimens are not normally desired because they do not have a gage

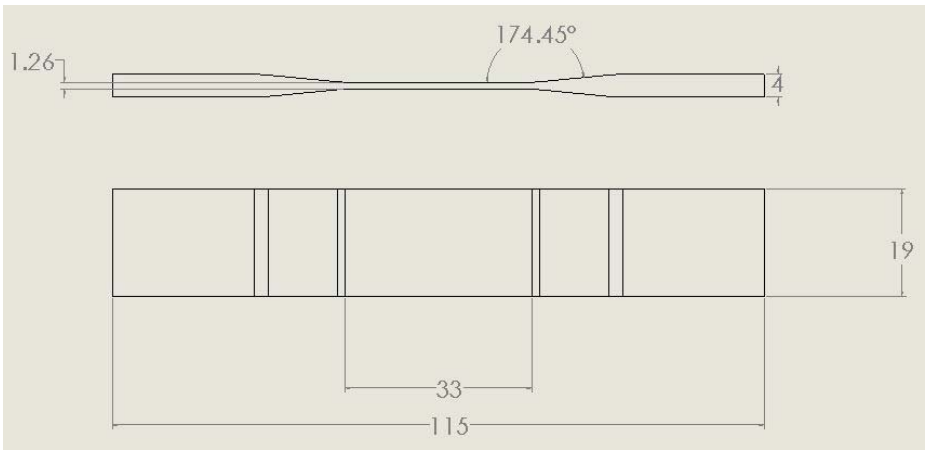

(a)

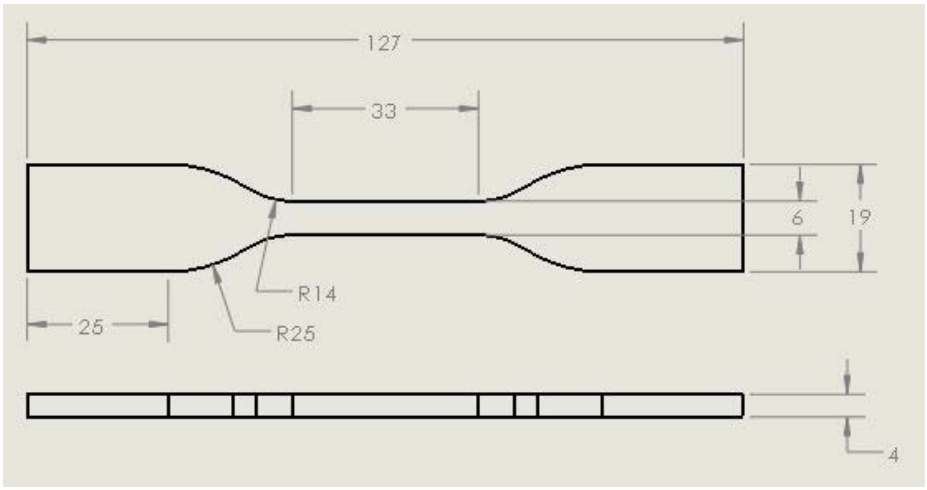

(b)

Figure 3.2. (a) Dimensions for YX tensile specimens. (b) Dimensions for ZX and XY tensile specimens.

section of reduced area. A gage section with a smaller area than the grip section is desirable to prevent slippage of the specimen during testing and to control where the failure occurs. If the grip section is wider, and therefore larger in area, more gripping surface is available and the specimen will likely break in the gage section before slippage in the grip section occurs. Since the joint layer is likely weaker than the rest of the specimen, it serves as a gage section where the failure will likely occur.

To print these specimens, half specimens were printed batches of 30 using the Fortus 450mc before the full specimens were printed. Full specimens were completed

by printing a case for the half part and then continuing the print after the half part was inserted into the case (see Figure 3.3). The Fortus 450mc has a function for integrating non-printed parts into printed parts. The user specifies a layer of the print for the Fortus 450mc to pause. During this pause, the print chamber can be accessed and other parts can be placed on the printed part to be integrated into the completed part. The print is then resumed and the part is completed.

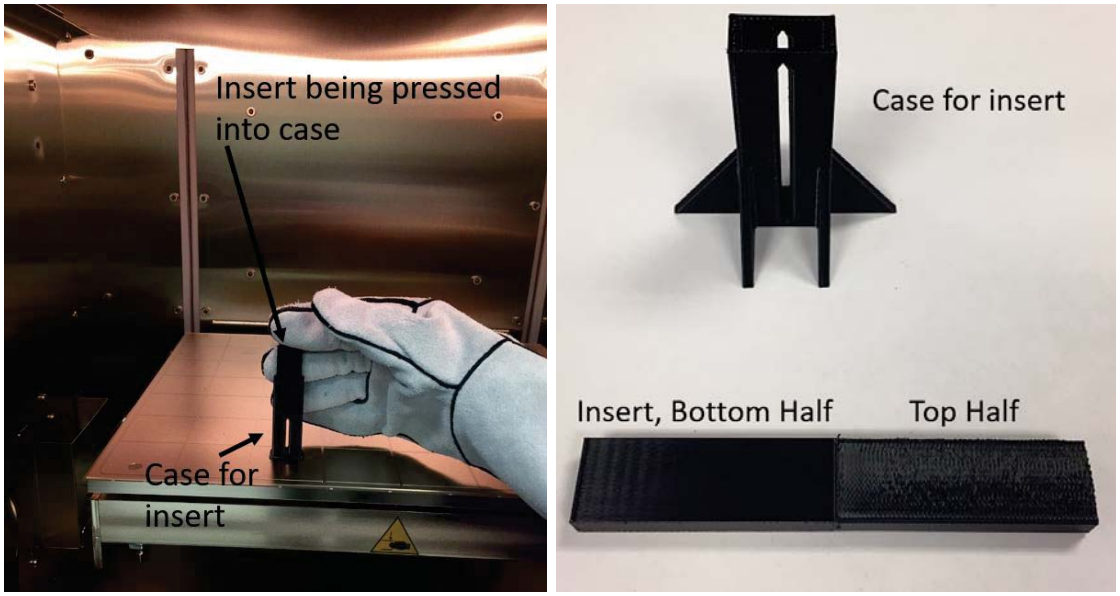

(a) **(b)**

Figure 3.3. (a) Inserting the pre-printed part into the case inside the Fortus 450mc during the pre-programmed pause. (b) Completed tensile specimen removed from case part. Note the right side of the specimen is newly printed in the ZX direction and the left side is the pre-manufactured insert part printed in the YX direction.

Column specimens completed in the LulzBot TAZ 6 were printed in a similar manner. The TAZ 6 was modified to print ULTEM 9085 by replacing parts allowing the printer to operate at a higher build volume temperature. An enclosure was constructed around the printer, and heat lamps controlled by a Watlow CV temperature controller were added to increase the build volume temperature (see Figure 3.4). The bulk of this work was accomplished by Cerri *et al.* [6], and modifications such as insulation and cooling for the hot end were added for this research. The case used

to hold the bottom half of the tensile specimen in place was printed separately and secured in the center of the build plate using high temperature Kapton tape (see Figure 3.4). The top half of the specimen was sliced in Repetier-Host V1.0.6 and the resulting G-code was edited. An offset was added to the G-code in the z direction to begin the print on top of the Fortus 450mc printed inserts. For specific procedures used to operate the modified TAZ 6, see Appendix A.

To manufacture a tensile column specimen in the TAZ 6, the insert was placed in the case after the auto-leveling process was completed. Inserts were stored in the build volume for at least 20 minutes before printing began to heat them to build volume temperature (see Figure 3.4). The build volume temperature at the start of the print was recorded along with the measured height of the printed insert. Images were captured using a FLIR Lepton v1.4 camera and a Raspberry Pi. The images were processed in Matrix laboratory (MATLAB) to produce a temperature profile of the part. Inserts were assumed to be at the build volume temperature and the nozzle was assumed to be at the nozzle temperature indicated by the TAZ 6. These temperatures were used as the maximum and minimum temperatures in the image for calibration in the MATLAB script. Images were taken when the nozzle was the same distance from the camera as the closest portion of the printed part so the intensity is appropriately scaled (see Figure 3.5). This method of obtaining the temperature profile in the modified TAZ 6, including the MATLAB script, was developed by Cerri *et al.* [6].

In addition to the tensile specimens manufactured using inserts, tensile specimens were also manufactured using a pause half-way through the print. This pause simulates printing on a pre-existing part by allowing the first half to cool to ambient temperature before resuming. A pause was inserted halfway through the print and the nozzle was moved away from the part throughout the pause. The G-code was

obtained by slicing the part in Repetier-Host V1.0.6 and then writing the pause into the resulting G-code. The modification to the G-code included movement in the Z then Y direction to move the nozzle away from the part, retraction of the filament to prevent it from seeping out of the nozzle, a five minute pause, and a re-priming of the filament before resuming the print. During the five minute pause, the hot end remains at printing temperature (355 C°). The filament seeps out during the pause despite the retraction of the filament, so the extrusion motor must be commanded to extrude near the end of the pause before the position is reset. Extruding filament near the end of the pause keeps feedstock primed when the print resumes. Attempts at normal air gaps failed (see Figure 3.6). The G-code was modified via MATLAB to obtain a negative air gap at the joint (see Appendix B). Half way through the G-code, every layer was shifted in the Z direction to achieve a negative air gap. A shift of -100μm was used first, resulting in a weak tensile specimen. A shift of -150μm was used next, resulting in a stronger tensile specimen. The coefficient of thermal expansion of ULTEM 9085 is 65.27 $\frac{\mu m}{m°C}$ [11]. With the half column parts measuring 28.75mm, the change in height after cooling 60 °C throughout the part is about 113μm. The coefficient of thermal expansion is likely the reason the nozzle has to be moved down at the joint layer in order to create a strong joint. After determining the offset required to achieve a good air gap at the joint layer, specimens were printed at build volume temperatures of 110 °C, 130 °C, 150 °C, 170 °C. At least five specimens were printed at each build volume temperature, and one print was used to manufacture all five any given temperature.

Specimens were originally built up to 57.5mm, the same height as the inserts used in the previous method of manufacturing tensile specimens. Many of the 57.5mm specimens failed near the grip rather than at the joint. This is a result of the stronger joint created with the pause print method. In the composite print method, the joint

could be counted on to fail and act as a gage section. The stronger joint created by the paused print method results in the specimen failing in the grips before the joint because of the extra stress applied in and near the gripped part of the specimen. Lighter grip pressures were tested, but slipping occurred in the grips. In an attempt to fix the problem, longer specimens were manufactured to provide a larger grip surface. A larger grip surface allows less grip pressure without slippage. The pause specimens used are 80mm in length, taking advantage of the entire wedge gripping surface.

Some composite specimens were printed cold, meaning that the inserted pre-existing part was at room temperature outside of the print chamber and then inserted into the case part before finishing the print. Others were printed hot, meaning the pre-existing parts were kept inside the print chamber while the case part was built. Leaving the pre-existing part inside the chamber allows it to reach a temperature assumed to be equal to the build volume temperature.

3.2.2 TAZ 6 Dogbone Tensile Specimens

The 80mm specimens also failed in the grip section, so the original type IV specimens from ASTM D-638 were printed. The type IV geometry was not used in the composite print method because inserts could not be precisely aligned, but the alignment using the pause method is as precise as possible since the nozzle position holds the same zero between the top and bottom halves. The modified TAZ 6 is not equipped with support material, so supports were designed in SolidWorks. When the print reached the gage section, the specimens were pulled around by the nozzle because of the small cross sectional area. The supports were designed to minimize the issue of the printed part moving under the nozzle. Dogbone specimens were printed in batches of five (see Figure 3.7). A band saw was used to cut the specimens apart and a Dremel tool was used to clean off excess material. The specimen to specimen

variation in width and thickness at the gage section for dogbone specimens printed in the TAZ 6 were more than 1%. The average gage section area was computed for each set of five specimens printed at a given build volume temperature.

Several attempts were often required to obtain an acceptable batch of tensile specimens. If defects were present in the gage section on multiple specimens in the batch, the specimens were discarded and another print was completed.

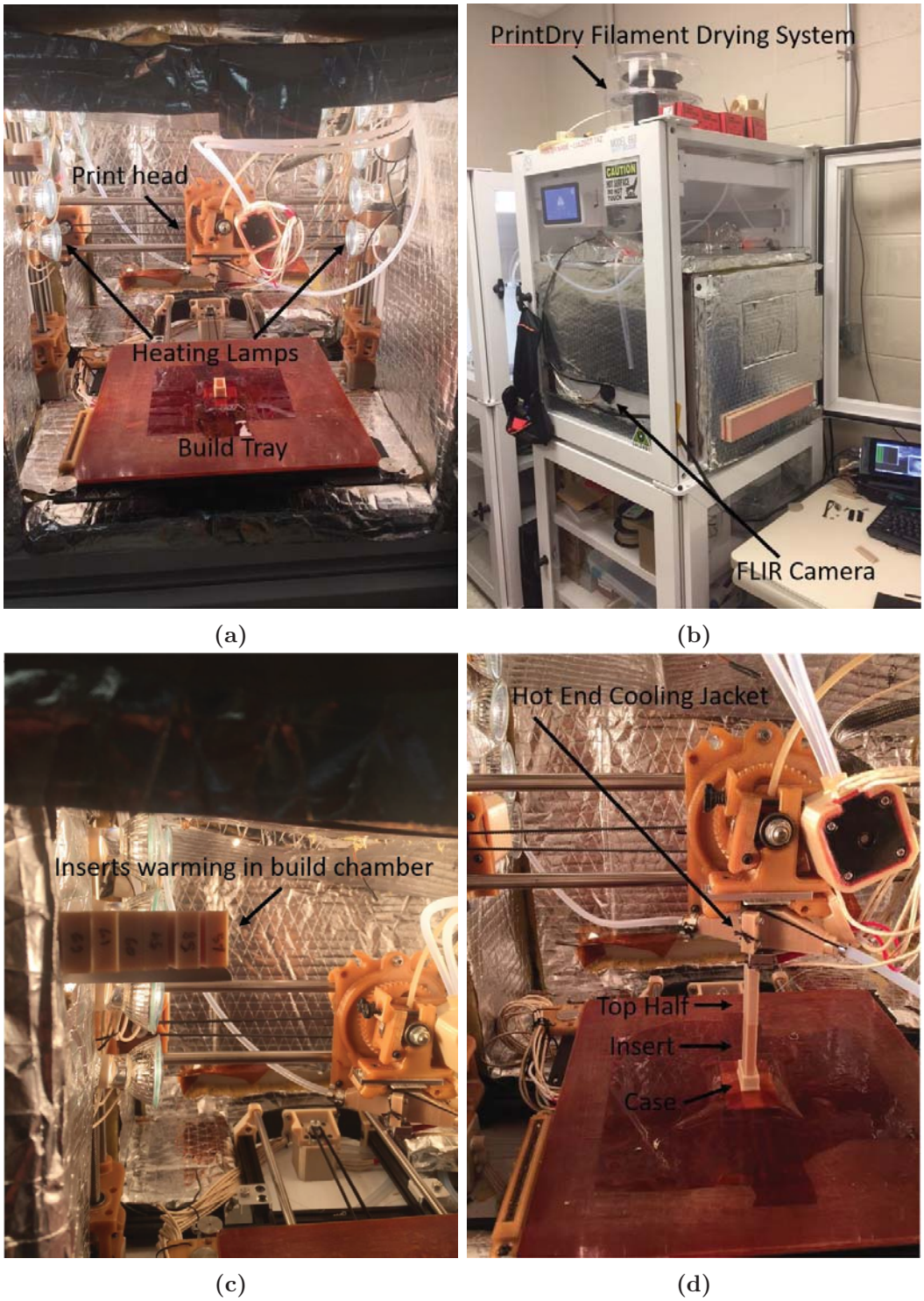

Figure 3.4. (a) Modified TAZ 6 interior. (b) Modified TAZ 6 exterior. (c) Shelf used to warm specimen inserts, note thermocouple in background at approximately the same height. (d) Composite column specimen being printed in in the TAZ 6.

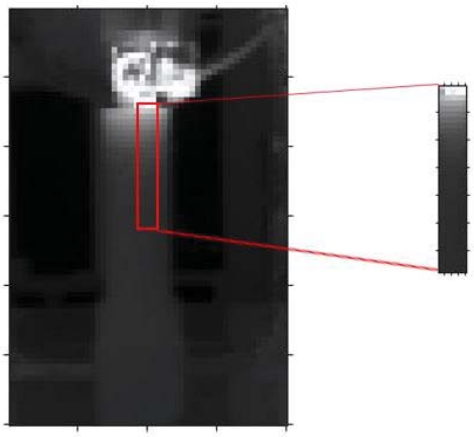

Figure 3.5. FLIR image (left) and cropped FLIR image (right) used to determine temperature profile of part during printing.

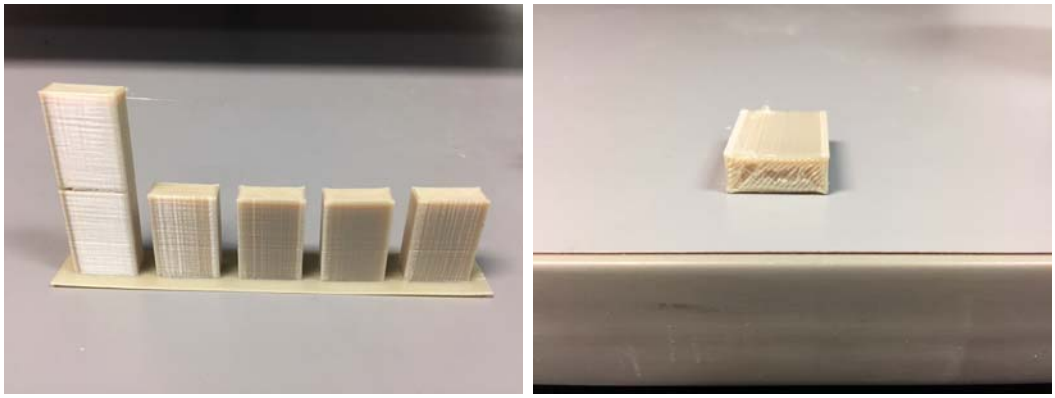

(a) **(b)**

Figure 3.6. (a) Lower half printed before the pause with normal air gap. Only one top half remained attached at the end of the print. (b) One of the top halves from the failed print. The layer making up the joint between the two parts did not make a strong bond and came off later in the print.

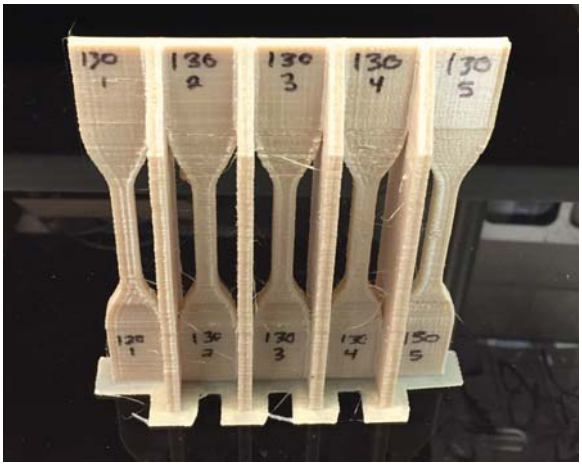

Figure 3.7. ASTM D-638 Type IV tensile specimens printed in the modified TAZ 6.

3.3 Compression Specimens

Prisms were manufactured in the Fortus 450mc to ASTM D695 specifications. Two print directions, ZX and XY were tested. A raster fill was used in both specimens, and the toolpath was set using Insight v.11.2 software.

3.4 Tensile Testing

Each tensile specimen was tested using a MTS Landmark 5-KIP machine. A MTS Extensometer, model 632.26F-20, was used in the gage section of each specimen. A 1 mm/min strain rate control was used for all specimens except the Stratasys printed YX specimens, where a strain rate of 5 mm/min was used. Strain rates were selected to achieve failure between 30 seconds and 5 minutes of testing. ASTM D638-14 states that the speed of testing should rupture the specimen between 0.5 and 5 minutes.

Marks were made on each specimen in the gage sections so the specimens are always gripped in the same place. Tabs mounted to the grip wedges are used to consistently grip the specimens without canting them. The center of the gage section was also marked so the extensometer could be mounted there. The extensometer is attached using rubber bands to the thin side of the gage section (see Figure 3.8). Care must be taken to prevent damage to the gage section by the knife edges of the extensometer. The size of the rubber bands used to mount the extensometer must not be small enough to damage the specimen, but must be small enough to hold the extensometer knife edges in place throughout the test. Once the specimen is gripped and the extensometer is mounted, the grip displacement, extensometer displacement, and force were offset. The tensile test was then started, and results from the tensile test were used to produce stress-strain curves and obtain mechanical properties.

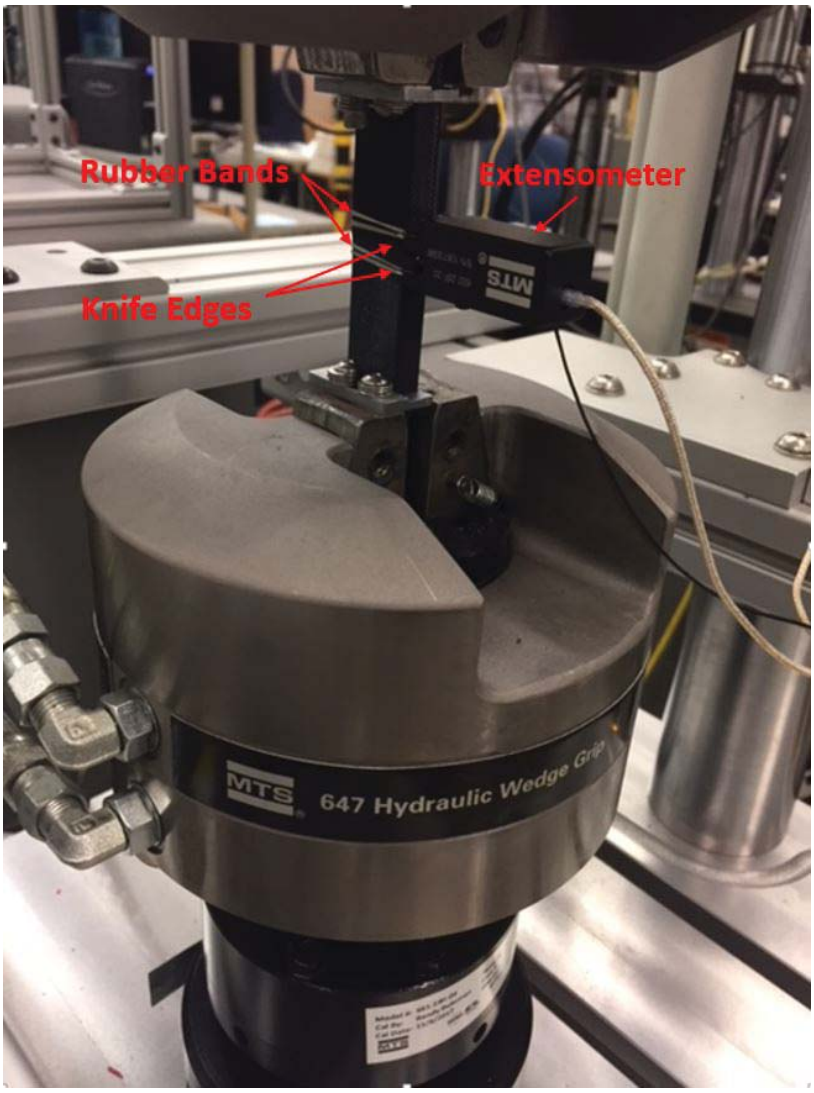

Figure 3.8. Extensometer Setup

3.5 Summary

The methods used to address the research objectives were laid out in Chapter III. Control tensile specimens were manufactured by a Fortus 450mc and at Stratasys to obtain baseline material properties to compare other specimens against. Column specimens and specimens manufactured with a pause were manufactured to test the strength of joints. The results of testing done on printed specimens are provided in Chapter IV.

IV. Results

4.1 Chapter Overview

This chapter contains the results of experiments conducted to address the research objectives. The first research objective is to validate the mechanical properties of ULTEM 9085 printed using FDM in different print orientations. The second research objective is to test joint strength between a pre-existing part and a newly printed part manufactured via FDM (the composite print method). The results of the testing done on normally printed specimens will be the standard that the composite print method results will be compared against. Results for specimens manufactured using the pause print method are also provided. In addition, thermal analysis was done to estimate the power required to heat the printed part to the desired build volume temperature in vacuum.

4.2 Tensile Tests

4.2.1 Stratasys Manufactured Tensile Specimens

Three different specimen geometries were tested (two dogbone specimen geometries and one column specimen geometry) and three separate FDM printers were used to manufacture the specimens. First, data were analyzed for the Stratasys printed specimens (see Figure 4.2 and Table 4.1). Each of the three specimen types was tested five times. The 2% offset method was used to determine yield strengths. Specimens printed in the YX direction had the highest strength, followed by XY and ZX specimens respectively. ZX and XY specimens broke at maximum stress. XY specimens have a fault in the gage section due to the nozzle path during printing, and all specimens failed at that point. A similar fault was observed by Bagsik *et al.* for specimens printed in that direction. The nozzle started and ended its path along the perimeter

in the gage section, allowing the filament to cool and resulting in a weak bond at that point (see Figure 4.1). The modulus of elasticity was higher for YX specimens than the others and about the same between YX and ZX specimens. Bagsik *et al.* also found that specimens were strongest printed in the YX, XY, and ZX directions respectively [4]. However, the modulus of elasticity is the same between the YX and ZX specimens in Bagsik's results. The higher ZX modulus found in Bagsik's research may be the result of a different raster fill or a different specimen geometry.

ZX specimens failed between layers in the gage section (see Figure 4.1). Failure between layers is expected in the ZX print direction because the tensile force is orthogonal to the layer direction. YX specimens exhibited a large elastic region (see Figure 4.2). The large elastic region in YX specimens can be attributed to the lack of a raster fill. The entire gage section consists of material laid in the direction of tensile force, so the force is resisted by strands of material rather than adhesion between roads or layers.

Table 4.1. Stratasys Tensile Specimen Data

Print Direction	XY	YX	ZX
Mean Ultimate Stress (MPa)	58.9	87.1	44.2
Ultimate Stress Standard Deviation	1.08	0.435	3.30
Ultimate Stress Coefficient of Variation (%)	1.83	0.499	7.47
Strain at Failure (mm/mm)	0.0917	0.415	0.0532
Strain at Failure Standard Deviation	0.00670	0.0165	0.00547
Strain at Failure Coefficient of Variaion (%)	7.30	3.97	10.27
Mean Yield Stress (MPa)	29.8	36.6	28.3
Yield Stress Standard Deviation	0.718	3.11	0.459
Yield Stress Coefficient of Variation (%)	2.40	8.50	1.62
Mean Modulus of Elasticity (GPa)	1.03	1.53	1.03
Gage thickness (mm)	4.14	1.33	4.22
Gage width (mm)	6.02	19.12	6.16
Speed of Testing (mm/min)	1	5	1

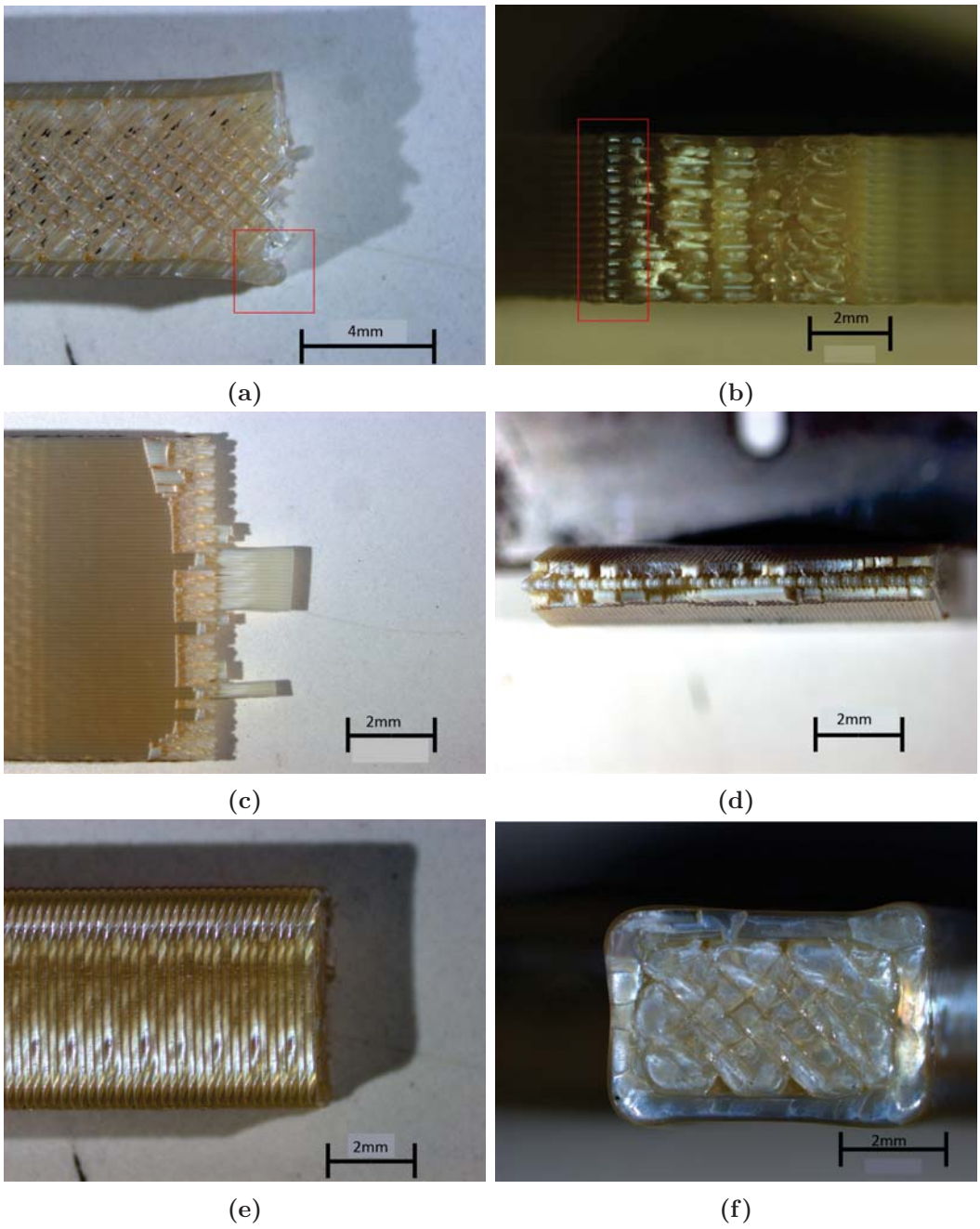

(a) (b)

(c) (d)

(e) (f)

Figure 4.1. Side and cross-sectional views at the point of failure on tensile specimens manufactured at Stratasys. (a) Side view of XY specimen failure location due to the nozzle path. Note there was no neck formation in the boxed section. (b) Cross sectional view of XY specimen (c) Side view of YX specimen (d) Cross-sectional view of YX specimen (e) Side view of ZX specimen (f) cross-sectional view of ZX specimen

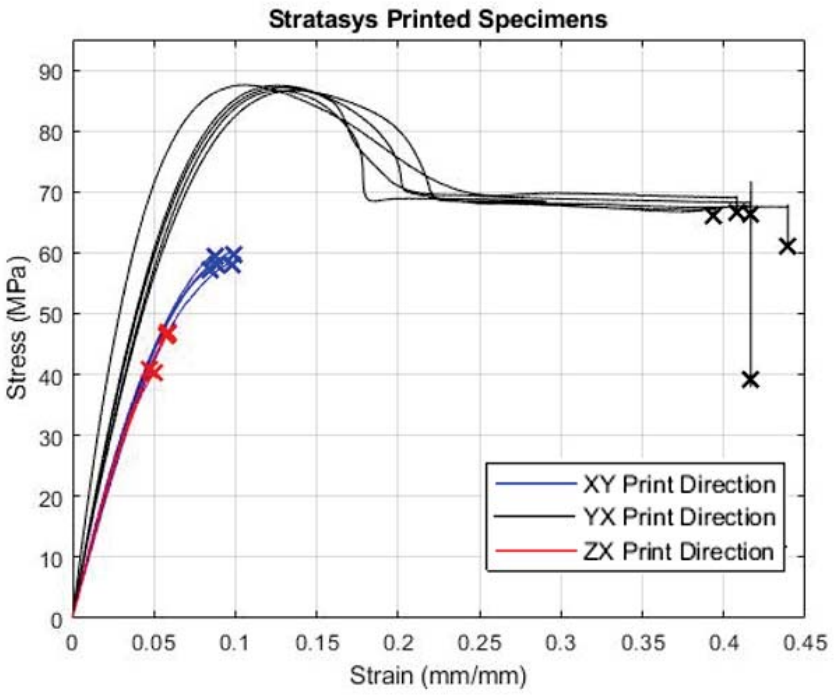

Figure 4.2. Stress-strain curves from specimens manufactured at Stratasys.

4.2.2 Composite Specimens

The data for ZX control specimens manufactured in the Fortus 450mc are shown in Table 4.2 along with Stratasys printed ZX specimens. Each specimen type was tested five times. A two-tailed t-test was done using the Stratasys dogbone mean ultimate strength as the assumed mean value. At a 95% significance level, the null hypothesis that the means are the same cannot be rejected for the column specimens but it can be rejected for the Fortus 450mc dogbone specimens. The Fortus 450mc column specimens can be considered part of the same distribution as the Stratasys specimens but the Fortus 450mc dogbone specimens cannot. These results demonstrate that column specimens manufactured in the Fortus 450mc have the same ultimate strength as Stratasys printed ZX specimens at a 95% significance level.

The results for all ZX specimens manufactured in the Fortus 450mc are summarized in Table 4.2. The 2% offset line did not intersect with the curve for cold

specimens, so the yield stress is listed as N/A. Specimens labeled "Cold" were manufactured using inserted parts left at room temperature prior to the print. Specimens labeled "Hot" used inserted parts left in the build chamber during the manufacture of the case, allowing them to reach the build volume temperature. For hot specimens, build volume temperature can be thought of as the same as part temperature at the start of the print. The composite specimens that were manufactured with pre-heated inserts had 65.8% the ultimate tensile strength of the column specimens while the strength of column specimens with inserts kept at room temperature prior to the print were 51.8% as strong. At a 95% significance level, the mean strength of the hot specimens is part of a different distribution than the mean of the cold specimens. These results suggest that the strength of the joint created using the composite print method depends on the temperature of the inserted part.

Table 4.2. Column Specimen Data

Specimen Type	Column	Dogbone	Cold Composite	Hot Composite
Mean Ultimate Stress (MPa)	45.2	41.3	23.1	29.8
Ultimate Stress Standard Deviation	3.21	1.36	1.78	0.721
Mean Yield Stress (MPa)	32.1	29.9	N/A	28.7
Yield Stress Standard Deviation	0.425	2.19	N/A	1.24
Mean Modulus of Elasticity (GPa)	1.06	1.06	1.02	1.06

The strength of column specimens manufactured in the TAZ 6 at various build volume temperatures are summarized in Table 4.3. Parts are left in the build volume to reach ambient temperature. Again, build volume temperature can be thought of as the same as part temperature at the start of the print. Four specimens were successfully printed and tested at 130 °C, five at 150 °C, and six at 160 °C. The mean ultimate strength increases as the build volume temperature increases, but the large standard deviation and number of samples make the results inconclusive. On a 90% confidence interval, the data from all three build volume temperatures tested can be

considered part of the same distribution.

Table 4.3. TAZ 6 Composite Column Specimen Data

Build Volume Temperature (°C)	130	150	160
Mean Ultimate Stress (MPa)	15.0	19.1	21.4
Ultimate Stress Standard Deviation	10.21	9.71	6.31

The variability is likely due to the placement of the inserted part prior to the print and the moisture content of the ULTEM 9085 filament. The height of each insert varied by ± 0.03 mm, enough to make a difference as was discovered when printing tensile specimens with a pause half way through the print. The inserts were not completely secured, and could move during the first few layers if the nozzle made contact with the inserts initially. In addition, the bed leveling process the TAZ 6 utilizes to obtain a zero for the nozzle introduces some variability. The large standard deviation shows how important process control is in creating a strong joint. Another possible factor is the moisture content of the inserts. The inserts were printed days before the tensile specimens were completed in the TAZ 6, giving them ample time to absorb moisture [12]. A high moisture content in the inserts could result in steam becoming trapped between the insert and the first layer of the new part. While the composite print method did not produce consistent results, it demonstrated the importance of alignment and air gap in the strength of the interlayer bond at the joint. To obtain more conclusive data, the pause method of printing column specimens was used.

Machined ULTEM was also tested since all other composite specimens were manufactured using a printed insert. ULTEM 9085 was only available in filament form, so extruded ULTEM 1000 was used. Inserts were machined from ULTEM 1000 and used to manufacture tensile specimens by printing ULTEM 9085 onto the inserts. The specimens were poorly attached despite using the same procedures as specimens manufactured with the printed ULTEM 9085 inserts. The different blend of ULTEM

is likely the cause of poor strength at the joint.

4.2.3 Joints Manufactured via Pause

To reduce variability in the manufacture of tensile specimens, a pause was used during the middle of the print to simulate printing on a pre-existing part. A pause was manually inserted halfway through the print and the nozzle was moved away from the part throughout pause. The G-code was modified via MATLAB to obtain a negative air gap at the joint layer. Half way through the G-code, every layer was shifted in the Z direction to achieve a negative air gap. A shift of -100μm produced weak tensile specimens and a shift of -150μm produced stronger specimens. A -150μm shift was used to manufacture all specimens with the pause method.

A pause of ten minutes was used to simulate printing on a pre-existing part with the 80mm specimens. Thermal images were captured during the pause with the 57.5mm specimens, where a pause of five minutes was used. The five minute period allowed the part to reach ambient temperature (see Figure 4.3). The top of the area captured is at the edge of the part, so it has a lower intensity. A maximum temperature of 145 °C and a minimum temperature of 125 °C was assumed for the cropped area. Bed temperature was set to 145 °C, and the heating from the bottom of the part can be seen in the plot. Since the top of the part is cooler than the middle, five minutes is sufficient to assume the top layers have cooled to ambient temperature. For added assurance that the part has had adequate time to cool to ambient temperature, a pause of ten minutes was used instead of five minutes for the 80mm tensile specimens.

The column specimens consistently failed in the grip section, so the type IV dog-bone geometry was used for the pause print method. The dogbone specimens printed in the TAZ 6 failed in the gage section, but none at the joint layer. The middle of

the gage section is where the pause was done during the print, so it is easy to tell if the failure occured at the joint layer. Reducing the air gap makes the joint at least as strong as other parts of the print. One possible contributing factor to these results is the number of specimens printed during one print. Since five specimens were printed at a time, the dogbones had more time to cool between layers than if one specimen was printed at a time. Each layer takes one minute and 37 seconds (slightly less time in the gage section layers). The part likely has time to cool close to ambient temperature between prints, especially in the gage section where there is a smaller cross section. An image was taken during a print at a build volume temperature of 170 °C in the gage section (see Figure 4.4). The figure shows that the part temperature is higher below the most recent layer, suggesting that the top layer has cooled to ambient temperature before the nozzle returns. A maximum temperature of 170 °C and a minimum of 160 °C were assumed for the cropped image. If the parts were cooled close to ambient temperature between layers, then the longer ten minute pause will have similar properties as all other layers. These results suggest that if the base part is heated to 170 °C, the joint will be as strong as the part being printed.

Since the failures did not occur at the joint layer, these data can be used to determine the relationship between strength and build volume temperature and to compare against specimens manufactured in the Fortus 450mc. Ideally, five specimens would have been tested for each build volume temperature. Due to print quality issues, sometimes multiple prints were tested for each build volume temperature. Five specimens were tested at build volume temperatures of 110 °C and 170 °C. Ten specimens were tested at build volume temperatures of 130 °C and 150 °C. One of the five tested at 170 °C was excluded from the data due to a print fault in the specimen that was determined to be a likely failure point before the tensile test was conducted.

Fracture surfaces of the specimens manufactured using the pause print method

can be seen in Figure 4.5. A clean failure between layers can be seen in each image, and there are not any significant differences visible between the fracture surfaces at different build volume temperatures.

The mean ultimate strength of specimens manufactured in the TAZ 6 at a build volume of 170 °C was 36.0 MPa and those manufactured in the Fortus 450mc (also at a set build volume temperature of 170 °C), was 41.3 MPa. In addition, the dimensional accuracy of specimens manufactured in the TAZ 6 was less than specimens manufactured in the Fortus 450mc. Ultimate tensile strength increased as build volume temperature increased with the exception of specimens printed at 150 °C (see Table 4.4 and Figure 4.6). Similarly, the standard deviation decreased as build volume temperature increased except for specimens printed at 150 °C.

The dip in the strength plot at 150 °C may simply be due to variability in print quality at build volume temperatures below 170 °C. Specimens with defects or batches with multiple defects were discarded, so major defects are likely not the cause of the dip in strength at a build volume temperature of 150 °C. Residual stresses could be present when a build volume temperature of 150 °C is used that are not present when printing at 130 °C and 170 °C. 3DX Tech, a supplier of ULTEM 9085 filament, recommends annealing completed parts in an oven at 150 °C to relieve stress [16]. Competing effects of increased neck growth as build volume temperature increases and residual stress could be the reason for the drop in strength at the 150 °build volume temperature. If the residual stress is a factor, it means that more residual stress occurs in parts printed at a build volume temperature of 150 °C than at the surrounding temperatures. Another reason the residual stress could be a factor is the time parts were left in the oven after printing in the TAZ 6. Prints were done overnight due to the long print time, so completed tensile specimens were removed from the oven some time the next day. The oven remained on until manually turned off, and

most specimens were removed from the oven hours after the print was completed. The different lengths of time left in the oven after the print was completed could have changed the residual stresses in the specimens and could be a reason for the drop in strength at build volume temperatures of 150 °C. It was expected that strength would increase as build volume temperature increases. Necks between roads have more time to develop the higher the build volume temperature is because it keeps the roads above their glass transition temperature for a longer period of time [13].

The standard deviation of strength at a build volume of 170 °C is an order of magnitude smaller than the other build volume temperatures tested. The small variability in strength of specimens manufactured at a 170 °C build volume temperature has important implications for validating FDM parts for use in aerospace applications. If build volume temperatures of less than 170 °C are used, a higher safety factor would need to be implemented in the design of components due to the higher standard deviation in strength. If design strength was based on three standard deviations from the mean, the design strength would be 20.5 MPa and 35.3 MPa for 110 °C and 170 °C respectively. The different temperature gradient between specimens in a batch may have had an effect, but the small standard deviation given by the specimens printed at a build volume temperature of 170 °C suggest that this effect was small.

Table 4.4. TAZ 6 Dogbone Specimen Data

Build Volume Temperature (°C)	110	130	150	170
Mean Ultimate Stress (MPa)	29.6	33.7	28.4	36.0
Ultimate Stress Standard Deviation	3.03	2.69	3.01	0.250
Ultimate Stress Coefficient of Variation (%)	10.2	7.98	10.6	0.695
Elastic Modulus (GPa)	0.966	1.02	0.903	0.987

The moisture content of the filament is also important. Three sets of dogbones were manufactured within one week of the spool of filament being replaced and stored in the PrintDry filament drying system. These dogbones were printed again at their

respective build volume temperatures after the filament was stored for more than two weeks in the PrintDry system. Specimens manufactured using filament that was stored for more than two weeks in the PrintDry system were stronger than those that were stored for less than one week (see Figure 4.7). Any filament used in orbit must be kept dry to obtain nominal strength of printed components. The moisture content of the filament was not measured, but Zaldivar *et al.* found that moisture levels of ULTEM 9085 filament above 0.4% result in weaker parts and that these moisture levels can be reached within one hour of room temperature exposure [12]. Zaldivar *et al.* measured moisture content by weighing filament after being exposed to humid environments and comparing to the dry weight of the filament [12]. In space, the moisture will likely not be an issue.

Density of column specimens manufactured via pause in the TAZ 6 at build volume temperatures of 130°C and 150°C were compared using computed tomography (CT) scanning. A Nikon XT H 225 ST was used to gather a series of X-ray images at different angles. A voltage of 142 kV and a current of 125μA were used to collect the images. In total, 720 images were collected, and each image was averaged four times. The effective pixel size that could be measured was 8μm. The images were reconstructed into a vgl file that could be analyzed using the Volume Graphics software package.

The porosity was 2.72% and 2.39% for build volume temperatures of 130 °C and 150 °C respectively. The higher build volume temperature resulted in a lower porosity. While only one sample was tested for each build volume temperature, the results align with what was expected. A higher build volume temperature means the filament spends a longer time above its glass transition temperature after being extruded, allowing more time for neck growth to occur [13]. For the specimen printed at a build volume temperature of 130°C, the porosity appears to be concentrated to a vertical

section on the right of the specimen as pictured (see Figure 4.8(a)). Porosity also seems to be concentrated in a vertical section of the specimen manufactured at a build volume temperature of 150°C (see Figure 4.8(b)). It can be seen from viewing the images from different orientations that the majority of the porosity is located in the raster filled interior of the specimens (see Figure 4.8(c)). A higher infill density and infill overlap may reduce porosity in the raster fill, the settings used for infill density and infill overlap can be seen in Appendix A.

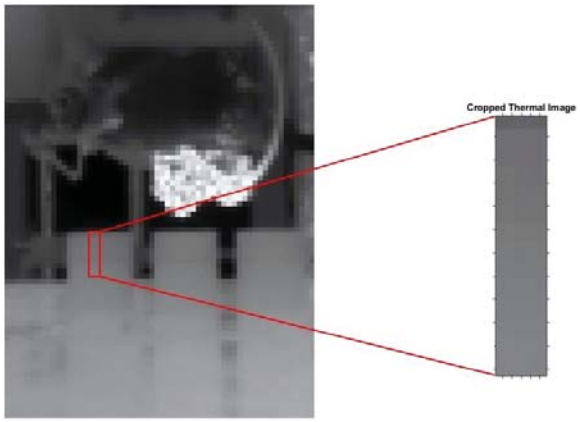

(a)

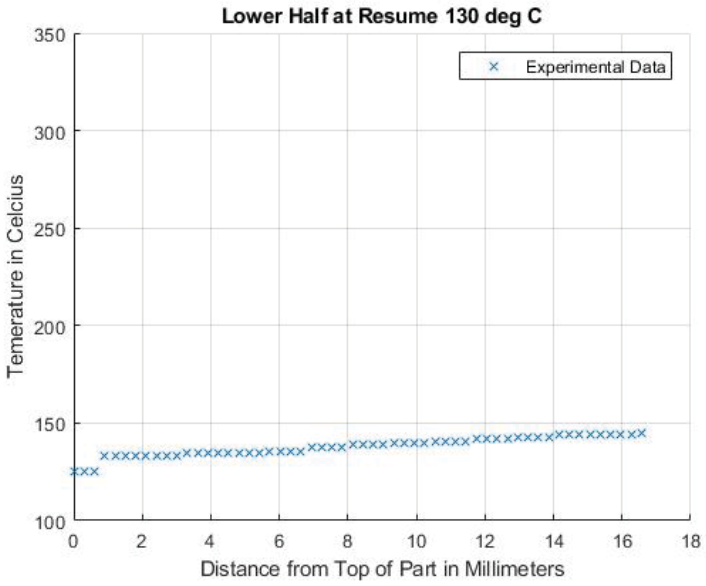

(b)

Figure 4.3. (a) Area cropped for analysis during a print done on column pause specimens. The print head is white in the image due to its higher temperature. Note the print head is moving to begin its first layer after the pause on the far left column specimen. (b) Temperature plot of designated area.

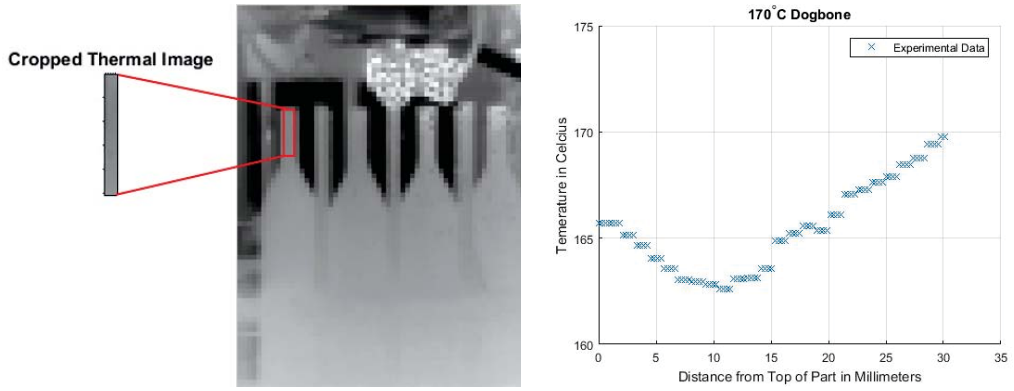

(a) (b)

Figure 4.4. (a) Area cropped for analysis from a print at a build volume temperature of 170 °C. The print head has moved left to right and is on its way back left in the image. (b) Temperature plot of designated area.

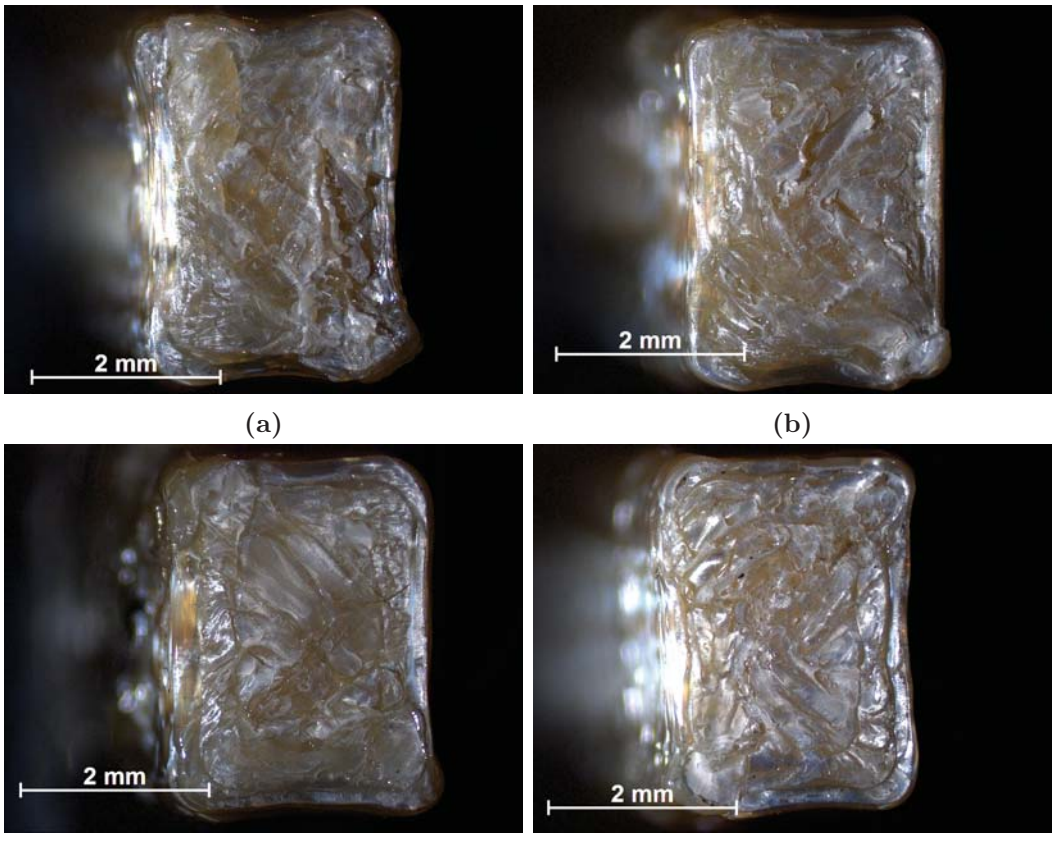

(a) (b)

(c) (d)

Figure 4.5. Cross-sectional views at the point of failure on tensile specimens manufactured in the modified TAZ 6 at the following build volume temperatures: (a) 110 °C (b) 130 °C (c) 150 °C (d) 170 °C. A clean failure between layers can be seen on each specimen pictured.

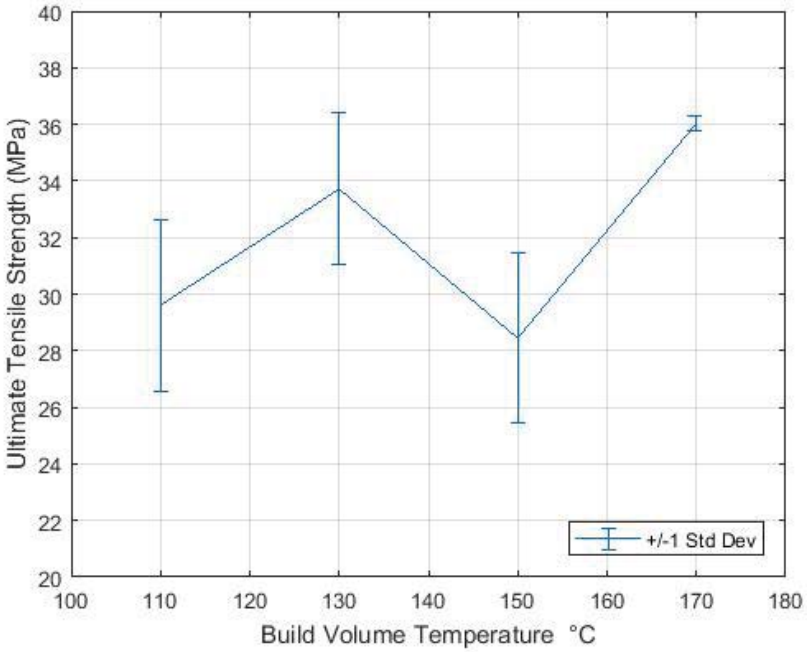

Figure 4.6. Ultimate tensile strength vs build volume temperature of dogbone specimens.

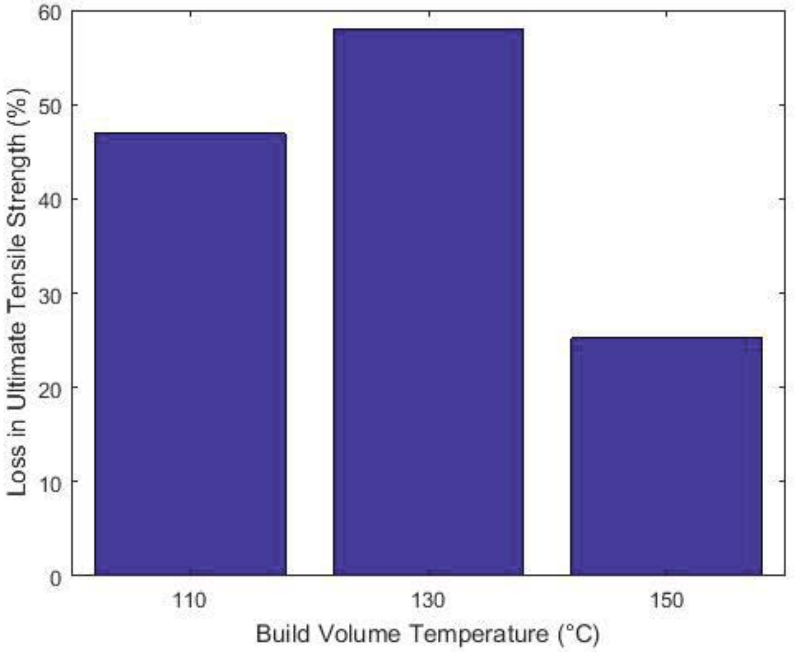

Figure 4.7. Percent loss of ultimate tensile strength of specimens using filament stored in a PrintDry filament drying system for more than two weeks and less than one week. Specimens made with filament dried in the PrintDry for more than two weeks were stronger at each build volume temperature than specimens dried for less than one week.

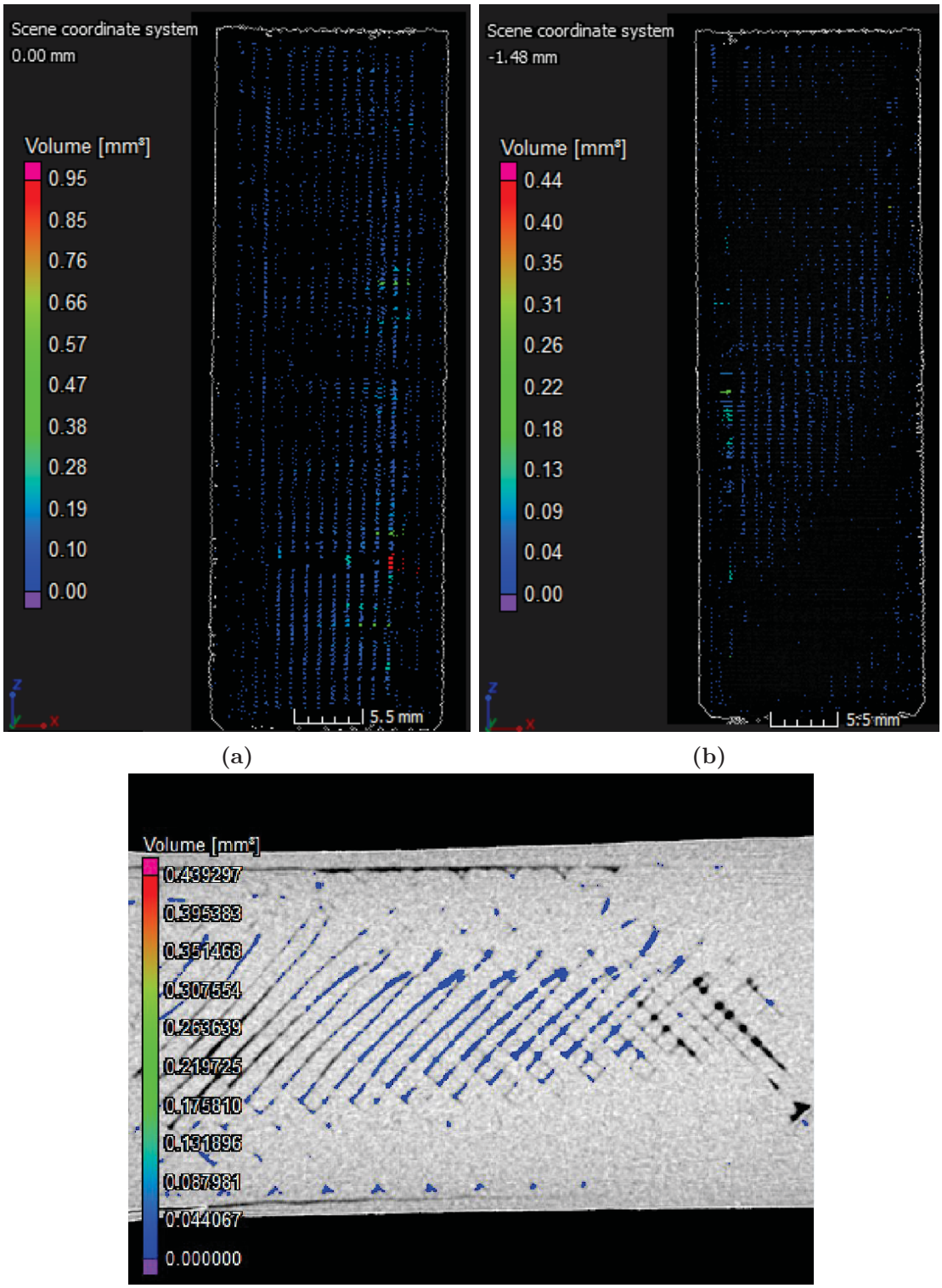

Figure 4.8. Images of column specimens manufactured via pause in the TAZ 6 taken using a Nikon XT H 225 ST Computed Tomography system. The amount of porosity in a particular part of the image is represented by its color. (a) Specimen manufactured at a build volume of 130 °C viewed from the side (b) Specimen manufactured at a build volume of 150 °C viewed from the side (c) Cross-section of specimen manufactured at a build volume of 150 °C

4.3 Thermal Analysis

To calculate the power required from lamps to achieve the desired part temperature in orbit, the methods that Cerri *et al.* developed were used [6]. First, the terrestrial thermal model developed by Cerri *et al.* was used to estimate the temperature profile of the part as it is being printed. Table 4.5 includes the values used in the model. The model assumes the layer height is the same as the nozzle diameter (0.4mm), constant material properties, and is steady state. Energy required for phase change was neglected along with temperature gradients in the X and Y directions (see Figure 4.9). Temperature in the Y direction is neglected because it is assumed there is negligible temperature change in within the 2mm thickness of the cylinder. Temperature in the X direction is neglected because the nozzle moves fast enough for differences in temperature in the X direction to be small. The 1D model does not capture interactions with the heated bed, so the part of the print used for experimental data is far enough away from the bed for this assumption to be accurate. The model is given by Equation 4.1 and is plotted against experimental data in Figure 4.11. T_0 is nozzle extrusion temperature in °K, T is ambient temperature in °K, z is distance down from the nozzle in meters, P is the circumference of the cylinder in meters, k is thermal conductivity of ULTEM 9085 in $\frac{W}{mK}$, and A_c is the cross sectional area of the cylinder in square meters (see Table 4.5). A new value of K is calculated for each increment (see Equations 4.1-4.3).

$$T(x) = (T_0 - T_\infty) \cdot e^{-mz} + T_\infty \tag{4.1}$$

$$m = \sqrt{\frac{KP}{kA_c}} \tag{4.2}$$

$$K = h + \epsilon\sigma(T^2 + T_\infty^2) \cdot (T + T_\infty) \tag{4.3}$$

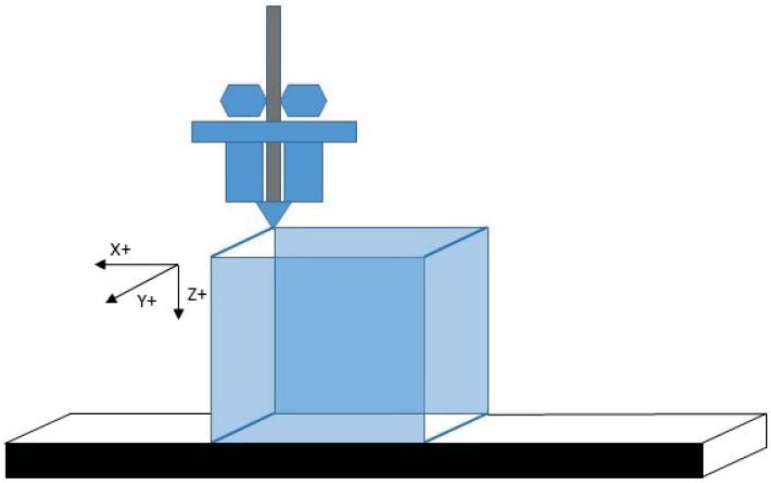

Figure 4.9. Coordinate system used in the thermal model. Figure from Cerri *et al.* [6].

Next, the cylinder that was used by Cerri *et al.* was printed in the modified TAZ 6 at a 170 °C build volume temperature and a print speed of 15 $\frac{\text{mm}}{\text{s}}$. Transience was neglected for the model, and the print speed of 15 $\frac{\text{mm}}{\text{s}}$ was best suited for this assumption out of the print speeds that were tested by Cerri *et al.* Thermal images were taken of the part as it was being printed. The thermal images were mapped to temperature using the fourth order scaling method used by Cerri *et al.* and by assuming the maximum temperature in the cropped image is the nozzle temperature and the minimum temperature is the build volume temperature (see Figure 4.10). The temperature profile of the part can be seen in Figure 4.11. The wide bars representing the experimental data in Figure 4.11 are a result of the resolution of the microbolometer FLIR camera. The nozzle distance was determined by counting the pixels of an object of known dimensions in the image and scaling appropriately. A two-term exponential was fit to the experimental data, and the slope of the exponential fit was used in the power requirement calculation.

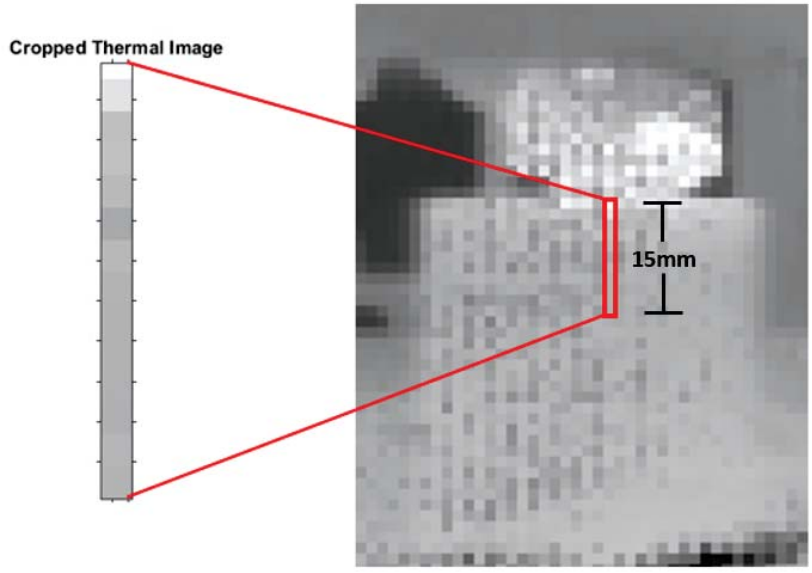

Figure 4.10. Thermal image of test cylinder printed at a build volume temperature of 170 °C.

Table 4.5. Values of terms used in the thermal model of a cylinder as it is being printed. These values are used in Equation 4.5

T_0	313 °C
T_{inf}	170°C
Emissivity (ϵ)	0.8
Perimeter (P)	308mm
Cross Sectional Area (A_c)	$2.5 * 10^{-7} m^2$
Thermal Conductivity (k)	0.25 $\frac{W}{mK}$
Convection Coefficient (h)	20 $\frac{W}{m^2 K}$

An energy balance was done for the orbital environment without a convection term (see Equation 4.4). The first term is radiation out of the part where T_∞ is assumed to be zero, the second is conduction into the top of the layer, the third is conduction out of the bottom of the layer, and the last term is energy stored in the printed part. T_0, the initial part temperature, is the average between the nozzle temperature and the temperature just below the nozzle determined by the FLIR microbolometer image data. The first two terms are evaluated using the slope of the experimental fit curve in Figure 4.11 at a distance of 0mm from the nozzle and 0.4mm (nozzle diameter and assumed layer height) from the nozzle respectively. The balance indicates that an

additional 0.7 $\frac{W}{cm^2}$ into the part is needed to achieve the desired temperature profile that resulted from a build volume temperature of 170 °C. If the temperature profile can be replicated in space, the strength between layers will likely be the same. The power requirement is a rough order of magnitude, as there was error in the energy balance done on the terrestrial model. Positive 0.3 $\frac{W}{cm^2}$, meaning additional power lost by the part, were unaccounted for in the terrestrial energy balance (see Equation 4.5). In other words, 0.3 $\frac{W}{cm^2}$ was the result of subtracting the energy storage term and the contribution from the lights from the left side of Equation 4.5. This indicates an additional 0.3 $\frac{W}{cm^2}$ needs to be added into the part for the energy balance to sum to zero. If the additional 0.7 $\frac{W}{cm^2}$ are supplied to the part while in the space environment by lamps or other means, the part quality will be the same as one printed in a 170 °C build volume.

$$\sigma\epsilon A_s(T_0^4 - T_\infty^4) - kA_c\frac{\partial T}{\partial z}\bigg|_{0mm} + kA_c\frac{\partial T}{\partial z}\bigg|_{0.4mm} = \rho C_p Vol\frac{\partial T}{\partial z}\frac{\partial z}{\partial t} \tag{4.4}$$

$$\sigma\epsilon A_s(T_0^4 - T_\infty^4) + hA_s(T_0 - T_\infty) - kA_c\frac{\partial T}{\partial z}\bigg|_{0mm} + kA_c\frac{\partial T}{\partial z}\bigg|_{0.4mm} = \rho C_p Vol\frac{\partial T}{\partial z}\frac{\partial z}{\partial t} \tag{4.5}$$

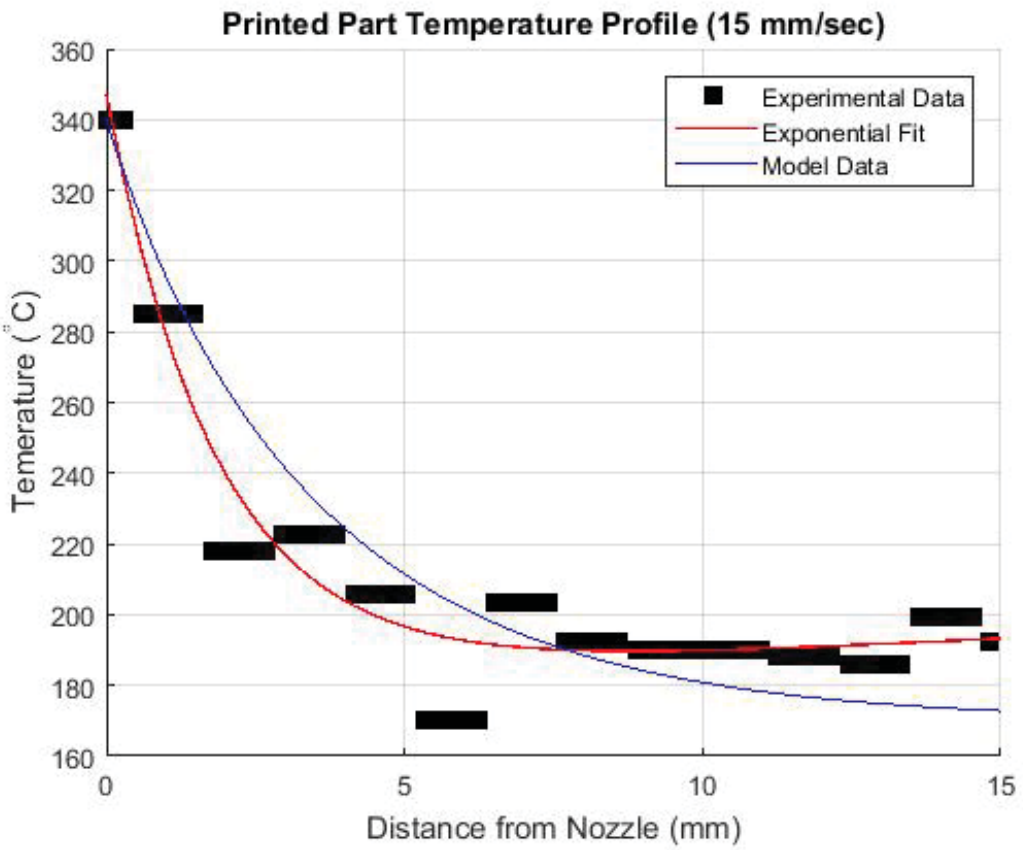

Figure 4.11. Thermal profile of hollow cylinder print at a build volume temperature of 170 °C.

4.4 Compression Tests

Tests were completed at 22-23 °C on a MTS 810 with a 110 kip load frame. The compression rate was 1.3 mm/min and specimens were compressed 15.4mm. Global strain is used, defined as the change in height divided by the overall original specimen height. Specimens manufactured in the ZX direction are stronger than those manufactured in the XY direction. XY specimens failed at 165.7 MPa (see Figure 4.12 and Table 4.6). ZX specimens did not fail, but continued to be compressed until the pre-determined final displacement of 15.4mm (see Figure 4.13). Failure in the XY specimens is a buckling outward from near the center. The gap is a result of the layers separating near the center, allowing the halves to buckle in opposite directions. These

findings are different than those of Bagsik *et al.* [4], where the research found lower compressive strengths and a failure mode for ZX specimens. The concave shape of the stress-strain curve after the yield point may be a result of the perimeter road and raster fill of the specimens in both print directions. Bagsik *et al.* also had a concave shape in the stress-strain curve for the ZX direction specimens, but not for the XY direction specimens. These differences may be attributed to printer settings such as layer height and air gap and the differences between the Fortus 450mc and Fortus 400mc used by Bagsik *et al.* The increasing stress seen in the ZX specimens after they separate from the YX specimens in the stress-strain plot is due to the increasing cross-sectional area as the ZX specimens are compressed.

The compression testing results show that parts printed in the XY direction will reach the ultimate tensile strength well before yield in compression. The compression yield strength is more than 1.5 times the ultimate tensile strength in the XY direction. It is expected that the tensile stress on one side of a beam in bending will be equal to the compression stress on the other, so only tensile strength needs to be considered in design for beam bending. In the ZX direction, yielding never occurs in compression, so tensile stress will be a larger concern than compression stress in ZX as well.

Table 4.6. Compression Specimen Data

	Mean Ultimate Stress (MPa)	Ultimate Stress Standard Deviation	Yield Stress (MPa)	Yield Stress Standard Deviation	Mean Elastic Modulus (GPa)
XY	166	2.97	92.4	1.24	1.93
ZX	N/A	N/A	91.8	1.32	1.65

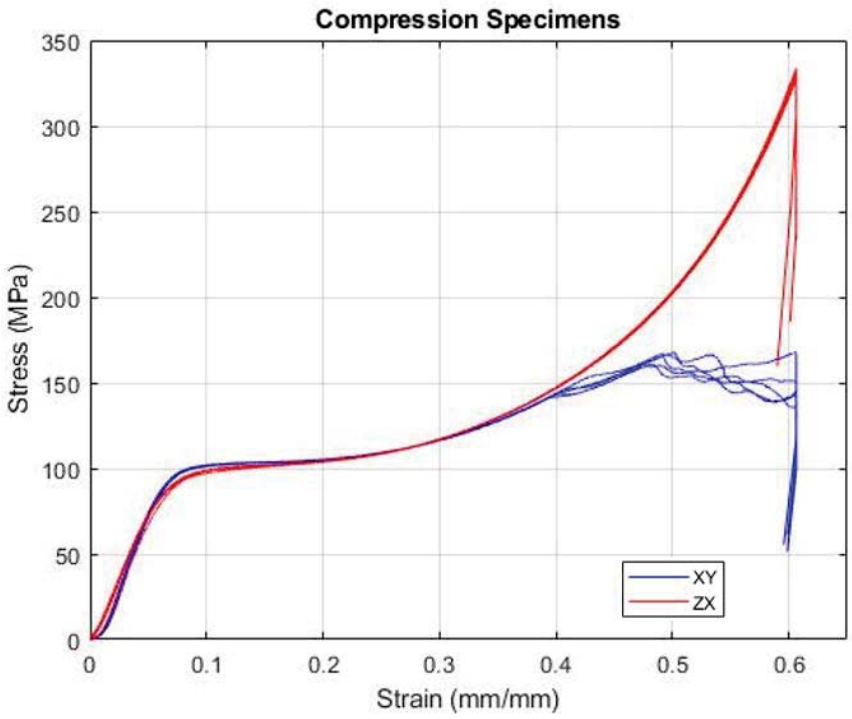

Figure 4.12. Stress-strain curves from compression specimens generated in MATLAB.

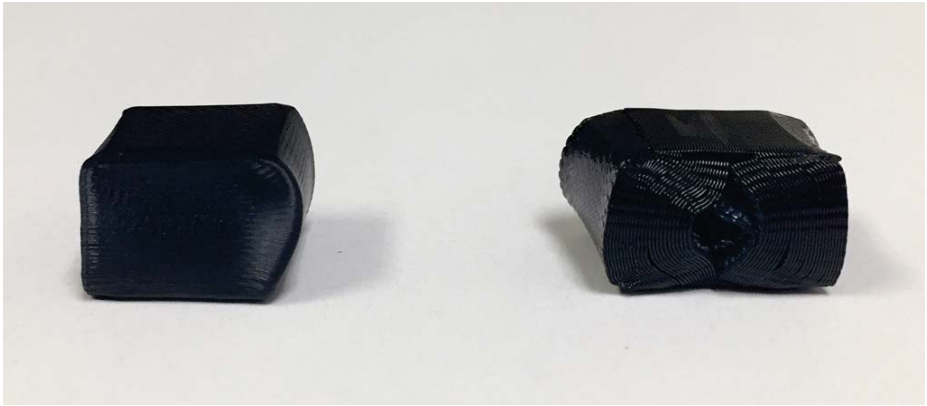

Figure 4.13. ZX compression specimen (left) and XY compression specimen (right).

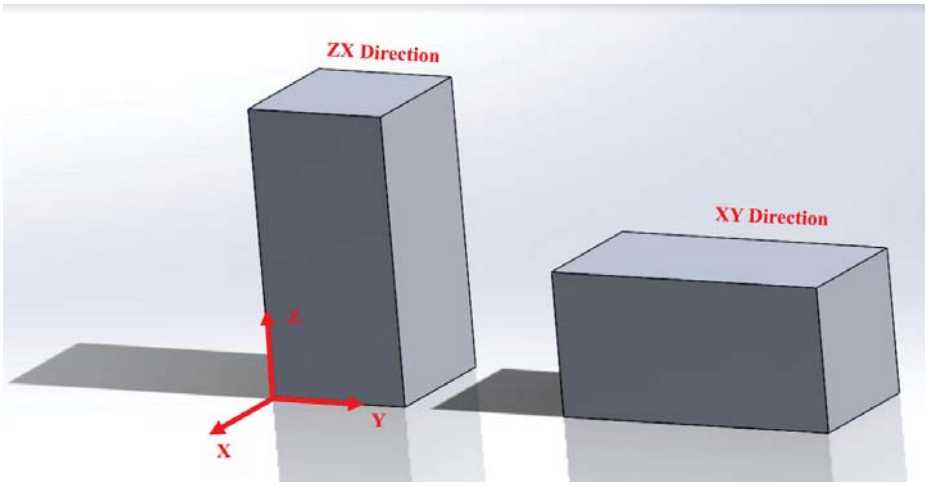

Figure 4.14. Compression specimen print directions.

4.5 Recommendations

To produce parts as close to nominal strength as possible, energy will need to be put into the part as it is being printed. The amount of energy put into the part while in the space environment is analogous to build volume temperature, and a 170 °C build volume temperature produced the strongest specimens. A heat lamp is one possible means of adding energy to the part.

When both the variables of alignment and air gap are fixed at their best, the joint is at least as strong as other parts of the print. The joint is at least as strong as other joints in the gage section because there was never a failure at the joint layer. If alignment alone is fixed, the joint is weaker. Alignment is as accurate as it will get when using the pause print method. When no changes were made to the air gap using the pause print method, the joint was weak. These findings will aid in determining requirements for an inchworm printer. One recommended requirement will define alignment accuracy and another will define air gap accuracy between layers. An inchworm printer would need to determine the print surface position with an accuracy on the order of tens of microns. Accuracy in the z direction on the TAZ 6 is 1.25 microns based on the stepper motor step angle and the pitch of the lead screws [17] [18]. The G-code specifies z position to the micron. The angle is also critical, so an inchworm would have to be carefully aligned orthogonally to the print surface. As the inchworm robot moves along the print, this accuracy must be maintained.

Another recommended requirement for an inchworm robot is a nozzle cleaning action. A nozzle wipe in between layers or between several layers will improve print quality and strength. Many of the faults in the dogbones printed on the modified TAZ 6 are a result of nozzle buildup that was dragged through material from previous layers. When the buildup drags on previous layers, it can remove material from the layer and reduce part strength and quality. The nozzle buildup grows until it is

stripped off, sometimes causing a print failure. These issues were not present in the specimens manufactured with the Fortus 450mc because it employs a nozzle wiping action between each layer.

A dovetail joint was also considered as an alternative to the composite print method. The dovetail joint would have a reduced usable cross-sectional area, and would be more difficult to manufacture. The nozzle would likely have to extrude material into the socket and would not be able to build a tail up layer by layer (see Figure 4.15). Assuming the most narrow part of the tail accounts for 40% of the surface area that could be used, the best strength that can be achieved is 40% of a column. The strength of a printed tail would likely be less than the joint built using the composite print method, and less reliable to manufacture.

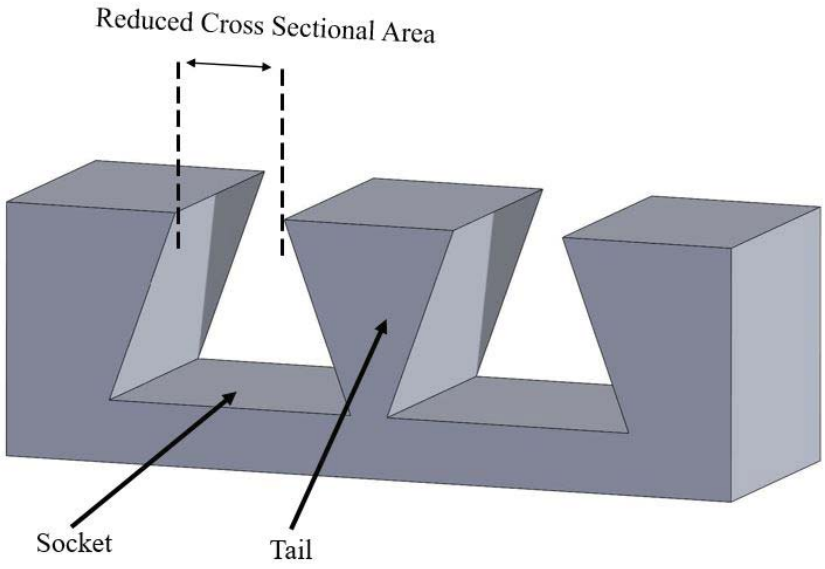

Figure 4.15. Illustration of dovetail joint.

4.6 Summary

Results from testing done to address the research objectives were laid out in Chapter IV. Tensile testing data showed that a strong joint can be made by printing

a new part on a base part using FDM if the air gap and build volume temperature are set properly. In addition, thermal analysis was used to estimate the amount of power needed to heat a part in vacuum to obtain the desired equivalent build volume temperature. Conclusions are given in Chapter V.

V. Conclusions and Recommendations

5.1 Summary

The problem of creating a joint between a new printed structure and a base structure can be resolved by heating the base structure and setting the proper air gap. If the base structure is heated to the desired build volume temperature, 170 °C, and the correct air gap is set at the base layer, the joint should be as strong as the rest of the printed part. The significance of the part temperature and air gap were discovered from the data from specimens manufactured using the pause print method. The air gap was varied until a strong joint was achieved and the build volume temperature was plotted against the ultimate tensile strength of pause print specimens. Further testing must be done on other aspects of the mobile FDM printer concept to determine its feasibility.

5.2 Conclusions

The goal of this thesis was to determine the feasibility of creating a joint between parts by fusing the base layer of a new part to a pre-existing part. It was found that if the air gap is properly adjusted, the joint layer is at least as strong as other layers in the part. None of the tensile specimens manufactured via the pause method failed at the joint layer. The composite print method demonstrated the importance of alignment and air gap in manufacturing a strong joint. If the nozzle is not properly aligned or the air gap is not set with an accuracy in the tens of microns, the joint will be made weak. Aligning the print axis to the base structure will be a difficult design problem for a mobile FDM robot.

Since the dogbones manufactured via pause did not fail at the joint layer, the data was used to determine a relationship between strength and build volume temperature.

Specimens manufactured at a build volume temperature of 170 °C were stronger than specimens manufactured at lower build volume temperatures. The strength of parts built at a 170 °C build volume temperature also exhibited a lower standard deviation in strength, meaning the parts are more consistent at that temperature. In space, it will be important to keep the part heated as it is being printed to achieve nominal strength. Constructing a build volume around the part is not feasible, so heat lamps are suggested as the means to heat the printed part in place of a heated build volume. It was estimated that an additional 0.7 $\frac{W}{cm^2}$ needs to be absorbed by the part being printed to achieve a temperature of 170 °C.

The mechanical properties of ULTEM 9085 printed in various print orientations were also determined. Results from these tests varied from others who have tested ULTEM 9085 printed in various print directions, but the trends of the data were largely in agreement.

It is recommended that the same blend of ULTEM is used between the base and the filament since the composite specimens manufactured with a ULTEM 1000 base and ULTEM 9085 filament were weak. A machined base would likely result in a bond at least as strong as a base manufactured via FDM, as long as the same blend of ULTEM is used between the base and the filament. In addition, the moisture content of ULTEM 9085 filament affects part quality and strength and must be kept in mind as the mobile FDM printer concept is developed.

5.3 Future Work

The composite print method should be revisited using inserts kept in a filament dehydration system. The moisture content of ULTEM 9085 filament affects strength, so the moisture content of the base part may also have an impact. In addition, a system capable of determining the position and orientation of the base part with

an accuracy on the order of tens of microns must be designed. More work needs to be done to determine the best air gap and other printer settings to use on the base layer. Zeroing the print head off of the base part is a difficult design problem, but is necessary in order to attach a new printed structure to a base structure with consistent joint strength.

The feasibility of using lamps to heat printed parts must also be investigated. In order to keep the printed part at the desired build volume temperature of 170 °C, testing should be done using heat lamps in vacuum.

Appendix A. Modified LulzBot TAZ 6 Information and Procedures

Specific procedures were required to print tensile specimens in the modified TAZ 6. An auto bed level is done at the beginning of each print to determine the nozzle position relative to the bed. The process is done by touching the nozzle to each corner of the bed. When the nozzle comes into contact with a corner, it is electrically grounded and the position is determined. For consistent prints, the nozzle must be clean during the automatic bed leveling process. Before each print, the nozzle was heated to 355 C°and then shut off. As soon as the TAZ 6 is shut off, a brass brush was used to clean the nozzle. If the power is on while brushing, the brush can cause a short.

The automatic bed leveling will also fail if any portion of the bed is grounded by something inside the print chamber. Aluminum backing for the insulation installed inside the print chamber can cause grounding issues, so it is important to keep the bed separated from the insulation.

To achieve good bed adhesion, Kapton tape is placed on the bed surface and the bed temperature is set to 145 C°. The Kapton tape was sanded by hand with 120 grit sand paper. A vacuum cleaner was used to clean the bed and chamber before each print. Over time the bed develops low and high spots, so extra tape must be placed in areas where the first layer does not adhere (see Figure A.1). A glue stick is not recommended to aid in bed adhesion because it is burned off when it comes into contact with the nozzle.

Printing at build volume temperatures above 130 °C in the TAZ 6 could not be accomplished until a cooling jacket was added to the B3 Innovations hot end. The problem was likely filament melting above the hot end, clogging the feeding system. A cooling jacket was added to the hot end to prevent this problem (see Figure A.2).

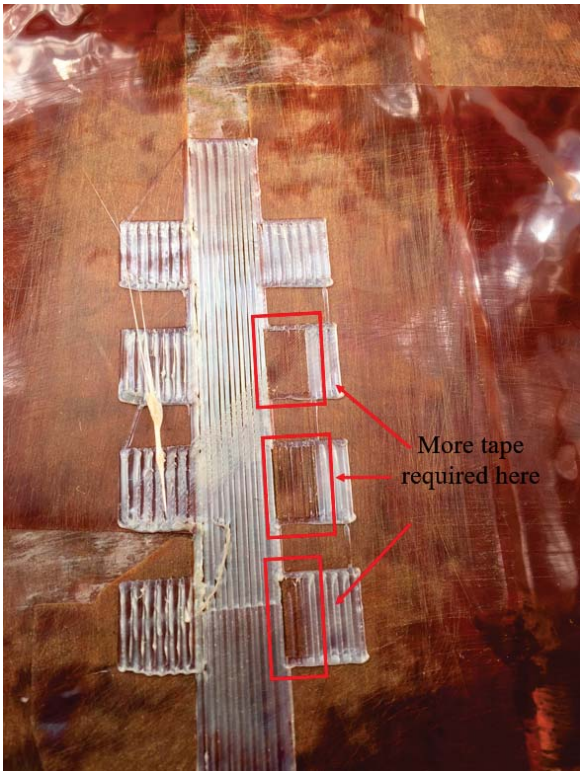

Figure A.1. First layer of raft, areas missing material require more Kapton tape for bed adhesion.

Pressurized air was ran through the cooling jacket via high temperature hose. After the addition of the cooling jacket, prints were completed at higher build volume temperatures.

Linear bearings also melted at a build volume temperature of 170 C°. The linear bearings that were originally installed on the TAZ 6 are made of a polymer, and the bearings mounted on the x-axis gantry melted. The original 12mm bearings were replaced with steel linear bearings. The z and y-axis bearings did not fail at 170 C°.

When printing type IV dogbone specimens to ASTM D-638 standards, the print must contain more than one dogbone. Attempts were made to print a single dogbone, but the gage section gets too hot and droops during the print. If more than one dogbone is printed at a time, there is adequate time for the previous layer to cool in the gage section before the next layer is added.

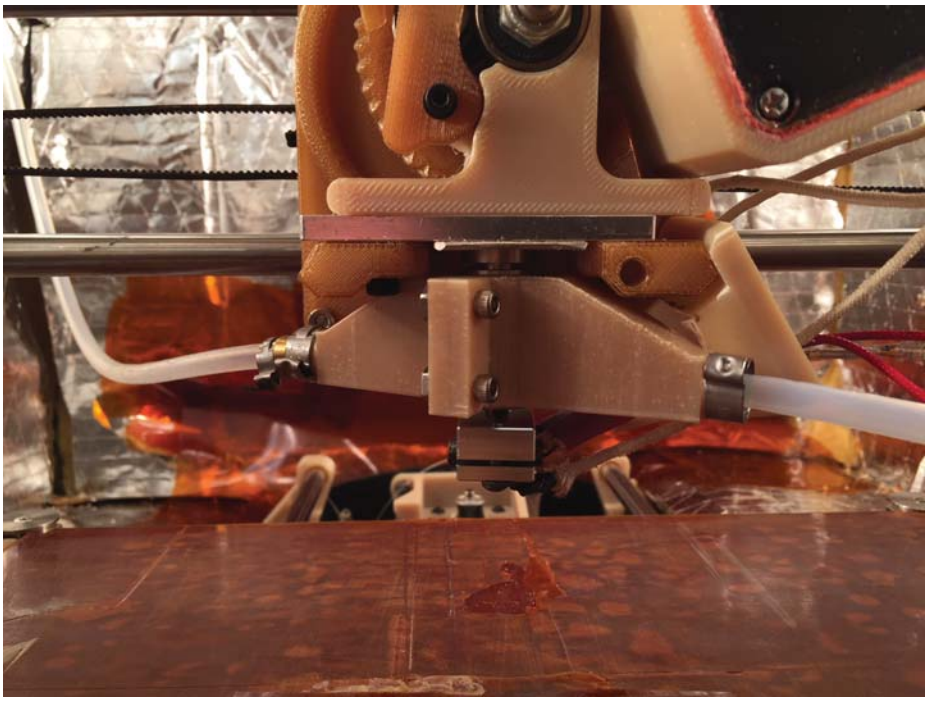

Figure A.2. Cooling jacket for the B3 Innovations hot end.

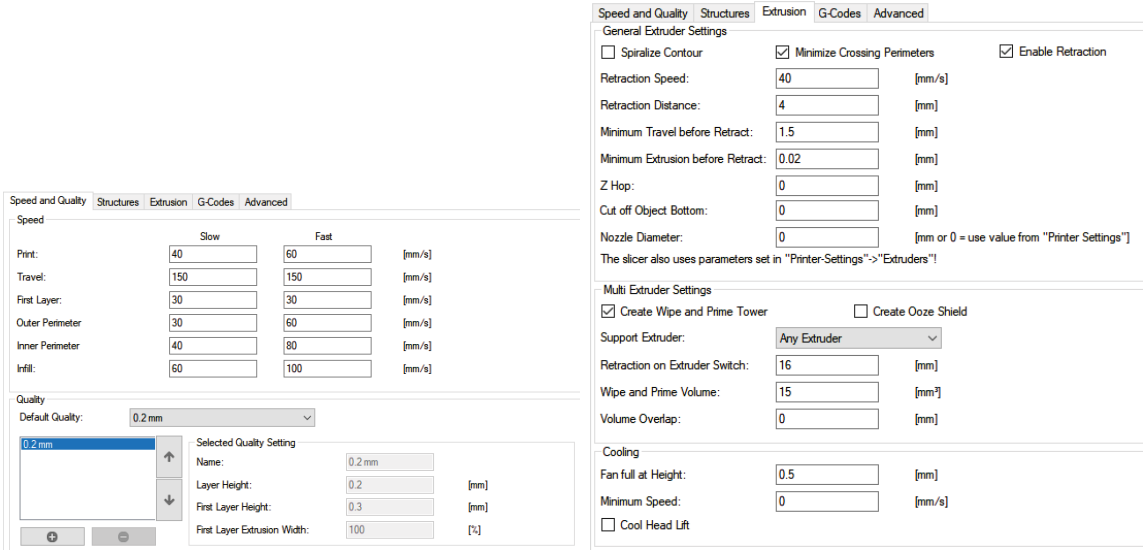

(a) (b)

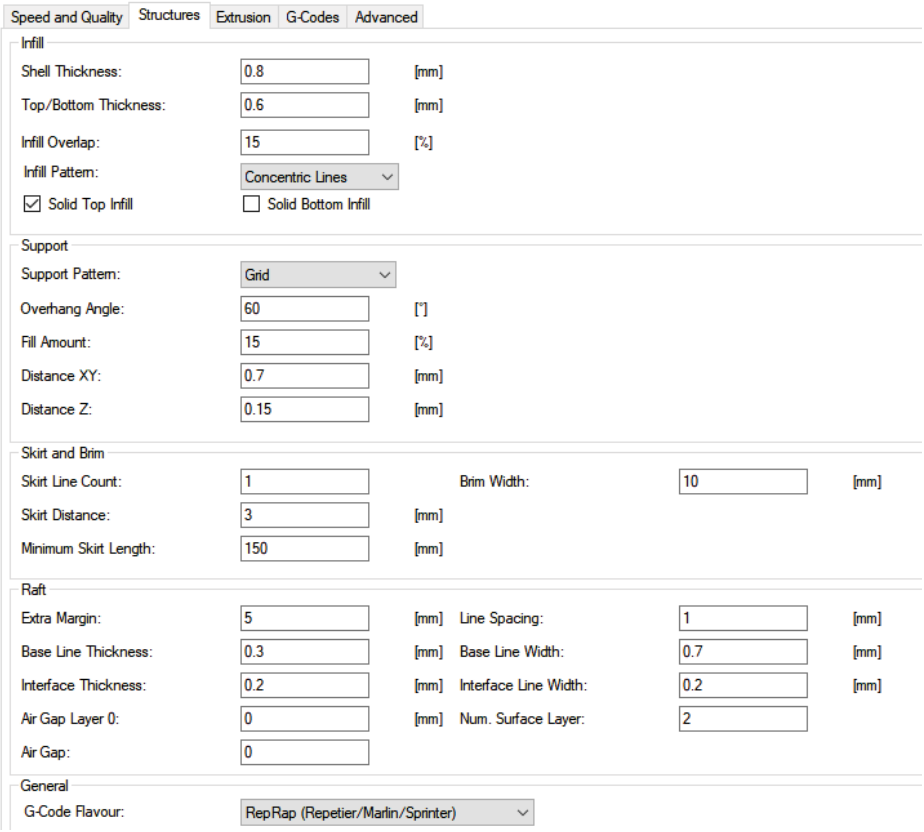

(c)

Figure A.3. CuraEngine Settings in Repetier-Host V1.0.6 used for all prints completed by the modified LulzBot TAZ 6 with the exception of the cylinder. (a) Speed Quality Tab (b) Structures Tab (c) Extrusion Tab

The following is a checklist for printing with the modified LulzBot TAZ 6:

1. Ensure all hoses are attached to their respective cooling jackets
2. Ensure all grounding wires, limit switch wires, and motor wires are connected (they frequently become loose or break)
3. Ensure print bed is clean and the right amount of Kapton tape is placed down and sanded at the print site
4. Set nozzle temperature to 355 °C and bed temperature to 135 °C manually
5. Once nozzle temperature reaches 355 °C, shut the printer off and clean the nozzle with a brass brush
6. Turn on heating lamps and set build volume temperature
7. Turn printer back on, connect printer to Repetier Host and start print
8. If the home button does not work, check button wires under bed
9. If auto bed leveling fails, ensure nozzle is clean, then check grounding wires under bed. If problem persists, check to see if insulation backing or anything else could be grounding the bed.
10. After auto bed leveling is completed, turn air on 1/16-1/4 of a turn (1/4 turn valve) as required. Too much air at low build volume temperatures will cool the nozzle and result in a print failure.
11. If base layer does not adhere to the print bed, add or remove Kapton tape as necessary, ensure Kapton tape is sanded

Appendix B. MATLAB Script for Editing G-Code

This MATLAB script was used to edit the G-Code to make a negative air gap at the joint layer. The layers were shifted down 0.15mm. There may be a G-Code command to re-zero the z-axis rather than using this MATLAB script to change the air gap at the joint layer.

G-Code editor

```
clear all; clc; close all;

filetext  = fileread('D638Clump2.txt');
expr = 'Z';
matches = regexp(filetext,expr,'match');
IND = strfind(filetext,'Z');
n = length(IND);
digits = 7;

for ii = 1:n
newIND(ii,1:digits) = [IND(ii)+1:IND(ii)+digits];
end

Zvals = filetext(newIND);
startvals = 11;
cutZvals = str2num(Zvals(startvals:n-2,1:digits));
shift = -.15;%distance to move Z axis in mm
newZvals = cutZvals+shift;
newSTR = num2str(newZvals,'%8.3f');
```

replace

```
fid = fopen('D638Clump2.txt','rt');
fin = fopen('D638ClumpEdit2.txt','wt');
S = fgetl(fid);
layer = 1;
while ischar(S)
    if length(S)>27
        if strcmp(S(27),'Z')

            if ~isempty(S) && strcmp(S(27),'Z')
                 if layer < 318
                     fprintf(fin,'%s\n',S);
                     layer = layer+1;
                 else
                     if layer<500%for str length

                        fprintf(fin,'%s\n',
[S(1:27),newSTR(layer,2:7)]);
                        layer = layer+1;
                     else
                        fprintf(fin,'%s\n',
[S(1:27),newSTR(layer,1:7)]);
                        layer = layer+1;
                     end
                 end
            else
                fprintf(fin,'%s\n',S);
            end
        else
```

```
            if ~isempty(S) && strcmp(S(28),'Z')
                 if layer < 318
                     fprintf(fin,'%s\n',S);
                     layer = layer+1;
                 else
                     if layer<500%for str length
                        fprintf(fin,'%s\n',
[S(1:28),newSTR(layer,2:7)]);
                        layer = layer+1;
                     else
                        fprintf(fin,'%s\n',
[S(1:28),newSTR(layer,1:7)]);
                        layer = layer+1;
                     end
                 end
            else
                fprintf(fin,'%s\n',S);
            end
        end
    else
             fprintf(fin,'%s\n',S);
    end

    S = fgetl(fid);
end
fclose(fid);
fclose(fin);
```

Published with MATLAB® R2017b

Bibliography

[1] TJ Prater, Qa Bean, RD Beshears, TD Rolin, NJ Werkheiser, Ea Ordonez, RM Ryan, Fe Ledbetter III, and George C Marshall. Summary Report on Phase I Results From the 3D Printing in Zero-G Technology Demonstration Mission, Volume I. 2016.

[2] Yong Zhou, Timo Nyberg, Gang Xiong, and Dan Liu. Temperature Analysis in the Fused Deposition Modeling Process. In *2016 3rd International Conference on Information Science and Control Engineering (ICISCE)*, 2016.

[3] Sung-Hoon Ahn, Michael Montero, Dan Odell, Shad Roundy, and Paul Wright. Anisotropic material properties of fused deposition modeling ABS. *Rapid Prototyping Journal*, 8(4):248–257, 2002.

[4] A Bagsik, V Schöppner, and E Klemp. FDM Part Quality Manufactured with ULTEM 9085.

[5] Additive Manufacturing Research Group. The 7 categories of Additive Manufacturing, 2014.

[6] Joshua Cerri. Fused Deopsision Modeling in an Orbital Environment, 2018.

[7] Aboma Wagari Gebisa and Hirpa G. Lemu. Investigating effects of Fused-deposition modeling (FDM) processing parameters on flexural properties of ULTEM 9085 using designed experiment. *Materials*, 2018.

[8] Timothy Philpot. *Mechanics Of Materials*. John Wiley & Sons, Inc, 2 edition, 2011.

[9] Cova Scientific. Polymer Outgassing and NASA Outgassing Standards, 2016.

[10] Technical report.

[11] Stratasys. Ultem 9085 Data Sheet.

[12] R. J. Zaldivar, T. D. Mclouth, G. L. Ferrelli, D. N. Patel, A. R. Hopkins, and D. Witkin. Effect of initial filament moisture content on the microstructure and mechanical performance of ULTEM 9085 3D printed parts. *Additive Manufacturing*, 2018.

[13] Cline Bellehumeur and Longmei Li. Modeling of Bond Formation Between Polymer Filaments in the Fused Deposition Modeling Process. *Journal of Manufacturing Processes*, 2004.

[14] A. Boschetto and L. Bottini. Accuracy prediction in fused deposition modeling. *International Journal of Advanced Manufacturing Technology*, 73(5-8), 2014.

[15] Nicolas G. Morales, Trevor J. Fleck, and Jeffrey F. Rhoads. The Effect of Interlayer Cooling on the Mechanical Properties of Components Printed via Fused Deposition. *Additive Manufacturing*, 2018.

[16] 3DX Tech. THERMAX PEI 3D FILAMENT, MADE USING ULTEM 9085.

[17] RepRap. NEMA 17 Stepper motor, 2018.

[18] LulzBot. Stainless Steel Lead Screw, 12mm x 420mm (x2).

REPORT DOCUMENTATION PAGE

Form Approved
OMB No. 0704–0188

1. REPORT DATE *(DD–MM–YYYY)*	2. REPORT TYPE	3. DATES COVERED *(From — To)*
21-03-2019	Master's Thesis	August 2018 — 21 March 2019

4. TITLE AND SUBTITLE

Manufacture of Fused Deposition Modeling Joints using ULTEM 9085

5a. CONTRACT NUMBER

5b. GRANT NUMBER

5c. PROGRAM ELEMENT NUMBER

6. AUTHOR(S)

Willburn Zane A. , Second Lieutenant

5d. PROJECT NUMBER

5e. TASK NUMBER

5f. WORK UNIT NUMBER

7. PERFORMING ORGANIZATION NAME(S) AND ADDRESS(ES)

Air Force Institute of Technology
Graduate School of Engineering and Management (AFIT/EN)
2950 Hobson Way
WPAFB OH 45433-7765

8. PERFORMING ORGANIZATION REPORT NUMBER

AFIT-ENY-MS-19-M-252

9. SPONSORING / MONITORING AGENCY NAME(S) AND ADDRESS(ES)

Undisclosed

10. SPONSOR/MONITOR'S ACRONYM(S)

N/A

11. SPONSOR/MONITOR'S REPORT NUMBER(S)

12. DISTRIBUTION / AVAILABILITY STATEMENT

DISTRIBUTION STATEMENT A:
APPROVED FOR PUBLIC RELEASE; DISTRIBUTION UNLIMITED.

13. SUPPLEMENTARY NOTES

14. ABSTRACT

The manufacture of joints between a base structure and a structure manufactured via Fused Deposition Modeling (FDM) will be investigated. ULTEM 9085, a high temperature plastic with potential aerospace applications, will be the material used. The specific application this research is focused on is a robotic and mobile FDM printer capable of building structures onto other structures in space. A joint will be formed by fusing the base layer of the printed structure and the surface of the base structure together. Tensile testing will be performed to determine the strength of the bond between parts. Tensile specimens will be manufactured with variable printer settings, including air gap and build volume temperature. In the orbital environment, lamps could be used to heat the part in place of a heated build volume. A thermodynamic model is used to estimate power required to heat the printed part in vacuum.
In addition, tensile and compression testing will be done on parts printed in various orientations to validate material properties. The material properties of specimens manufactured under normal conditions will be the standard that printed joints will be compared against.

15. SUBJECT TERMS

Ultem 9085; Fused Deposition Modeling; Build Volume Temperature

16. SECURITY CLASSIFICATION OF:			17. LIMITATION OF ABSTRACT	18. NUMBER OF PAGES	19a. NAME OF RESPONSIBLE PERSON
a. REPORT	b. ABSTRACT	c. THIS PAGE			Carl R. Hartsfield, PhD , AFIT/ENY
U	U	U	UU	87	19b. TELEPHONE NUMBER *(include area code)* (937)255-3636, x4542; carl.hartsfield@afit.edu